

RESEARCH

Open Access



# Evaluation of extra virgin olive oil compounds using computational methods: in vitro, ADMET, DFT, molecular docking and human gene network analysis study

Velid Unsal<sup>1\*</sup> , Reşit Yıldız<sup>1</sup>, Aziz Korkmaz<sup>1</sup>, Başak Doğru Mert<sup>2</sup>, Cemile Gunbegi Caliskan<sup>3</sup> and Erkan Oner<sup>4</sup>

## Abstract

This study investigates the phenolic compounds (PC), volatile compounds (VC), and fatty acids (FA) of extra virgin olive oil (EVOO) derived from the Turkish olive variety "Sarı Ulak", along with ADMET, DFT, molecular docking, and gene network analyses of significant molecules identified within the EVOO. Chromatographic methods (GC-FID, HPLC) were employed to characterize FA, PC, and VC profiles, while quality parameters, antioxidant activities (TAC, ABTS, DPPH) were assessed via spectrophotometry. The analysis revealed a complex composition of 40 volatile compounds, with estragole, 7-hydroxyheptene-1, and 3-methoxycinnamaldehyde as the primary components. Hydroxytyrosol, tyrosol, oleuropein, apigenin, ferulic acid, and vanillic acid emerged as main phenolic constituents, with hydroxytyrosol and apigenin exhibiting high bioavailability. Molecular docking highlighted oleuropein and pinosresinol as compounds with strong binding affinities, though only hydroxytyrosol, apigenin, and pinosresinol fully met Lipinski and other drug-likeness criteria. DFT analysis showed that oleuropein and pinosresinol have notable dipole moments, reflecting polar and asymmetrical structures. KEGG enrichment analysis further linked key molecules like oleuropein and apigenin with pathways related to lipid metabolism and atherosclerosis, underscoring their potential bioactivity and relevance in health-related applications.

**Keywords** EVOO, Sarı Ulak, ADMET, DFT, Molecular docking, Gene network analysis

## Introduction

The olive tree (*Olea europaea L.*), one of the earliest cultivated species, is predominantly found in Mediterranean countries, where Spain, Italy, Greece, and Turkey are among the leading producers. Extra virgin olive oil (EVOO), obtained from olive fruit by mechanical or physical processes it is considered the highest quality in olive oil classification due to its pleasant flavor and health benefits [1–3]. As it is derived directly from olives essentially pure olive juice-quality assessments of EVOO focus on components such as phenolic and pigment profiles, which contribute to its sensory attributes and pharmacological effects. Additionally, to be classified as EVOO, the

\*Correspondence:

Velid Unsal  
velidunsal@artuklu.edu.tr

<sup>1</sup> Department of Nutrition and Dietetics, Faculty of Health Sciences, Mardin Artuklu University, 47100 Mardin, Türkiye

<sup>2</sup> Energy Systems Engineering Department, Engineering Faculty, Adana Alparslan Türkeş Science and Technology University, 01250 Adana, Türkiye

<sup>3</sup> Department of Medical Services and Techniques, Vocational Higher School of Health Services, Mardin Artuklu University, 47100 Mardin, Türkiye

<sup>4</sup> Department of Biochemistry, Faculty of Pharmacy, Adiyaman University, Adiyaman 02000, Türkiye



© The Author(s) 2025. **Open Access** This article is licensed under a Creative Commons Attribution-NonCommercial-NoDerivatives 4.0 International License, which permits any non-commercial use, sharing, distribution and reproduction in any medium or format, as long as you give appropriate credit to the original author(s) and the source, provide a link to the Creative Commons licence, and indicate if you modified the licensed material. You do not have permission under this licence to share adapted material derived from this article or parts of it. The images or other third party material in this article are included in the article's Creative Commons licence, unless indicated otherwise in a credit line to the material. If material is not included in the article's Creative Commons licence and your intended use is not permitted by statutory regulation or exceeds the permitted use, you will need to obtain permission directly from the copyright holder. To view a copy of this licence, visit <http://creativecommons.org/licenses/by-nc-nd/4.0/>.

oil must have a free acidity level no higher than 0.8% and must be free from sensory defects [1–3].

The positive health impacts of EVOO consumption, particularly in reducing cardiovascular and metabolic disease risk, are largely attributed to its fatty acid content and phenolic compounds [4, 5]. Fatty acids, which make up ~ 97–99% of EVOO's total weight, primarily include unsaturated fats like oleic acid, linoleic acid, and palmitoleic acid, along with around 14% saturated fats such as palmitic and stearic acids. The remaining fraction (1–3%) consists of bioactive compounds like phenols, phytosterols, tocopherols, and squalene [2, 6]. Numerous studies have highlighted the antioxidant, antimicrobial, and anti-inflammatory properties of EVOO's phenolic compounds, underscoring their significance in health-related research [7]. To date, at least 36 phenolic compounds have been identified in EVOO, with compositions varying from 0.02 to 600 mg kg<sup>-1</sup>, influenced by factors like region, olive variety, genetic variations, environmental and climatic conditions, maturity at harvest, storage, and oil extraction methods [8–11]. Given the complex and variable composition of EVOO, advanced computational methods have become essential for accurately assessing and predicting the bioactivity of its diverse compounds.

Recent advancements in computational modeling, grounded in artificial intelligence (AI) and machine learning, have transformed research into chemical compound identification, target prediction, and toxicity assessment. Computational methods like virtual screening and molecular docking facilitate efficient drug discovery by reducing time and costs associated with experimental procedures. This shift allows researchers to screen for potential therapeutic agents, monitor drug efficacy, and explore drug repositioning strategies [12–14]. In EVOO studies, such approaches can provide insights into the bioactivity of particular compounds, allowing for more detailed analysis across varieties, geographical regions, and preparation conditions.

In this study, PC, VC, FA, antioxidant and antimicrobial analyzes of an EVOO obtained from a Turkish olive variety, as well as the evaluation of important molecules detected in EVOO with computer-based programs (ADMET, DFT, Molecular Docking and Gene network analysis) were performed. The olive oil evaluated in this study was first proven by laboratory findings to be EVOO. Then, it was supported by computer-based studies. This is an indication that the study is original. Previous studies on olive oil have predominantly been conducted on topics such as variety, growing conditions and authenticity. In this study, in addition to a comprehensive quality assessment of a characteristic EVOO of a common Turkish olive variety, the evaluation of its major phenolic compounds was also carried out using computer-based

programs including ADMET, DFT, molecular docking and gene network analysis.

## Materials and methods

### Chemicals

The chemicals used were of analytical purity and the standards used (tyrosol, oleuropein, pinoselinol, caffeic acid, syringic acid, vanillic acid, p-coumaric acid, ferulic acid, gallic acid, luteolin, hydroxytyrosol, apigenin) were of high purity (purchased from Sigma-Alrich).

### Olive fruits

Olives of the Sarı Ulak variety were used in the EVOO production. The fruits of this olive were collected and purchased from a farmer's garden in Çakırlı Village. (Tarsus County, Türkiye). The geographical location of this garden is illustrated in Fig. 1. The olives were harvested during the first week of November in the 2023 season and were classified as maturity level category 2, according to the International Olive Council (IOC, 2011) [15]. At this maturity stage, one side of the olive changes from yellow to pink or reddish. Approximately 100 kg of olives were harvested and transported to the olive oil mill facility for processing on the same day.

### Extraction of EVOO

EVOO was extracted using a boutique-scale olive oil mill (SLN-OLV200 Machine, Selni Makina, Istanbul, Turkey). This machine was designed to perform leaf-sorting, washing, crushing, malaxation, decantation and separation processes. In addition, its malaxator had a closed system that could hold the nitrogen gas pressed into it. Nitrogen gas can prevent quality defects by minimizing oxidation in the olive oil during the malaxation process. In the extraction of EVOO, malaxation process was at 26 ± 1 °C for 30 min. The EVOO taken from the separator was placed in 100 ml amber bottles and stored at 4 °C until analysis.

### Quality parameters analysis in EVOO

FFA, PV and extinction coefficients ( $K_{270}$  and  $K_{232}$ ) of the EVOO were measured according to the Turkish Official Methods (2014). FFA and PV were expressed as % oleic acid and meq O<sub>2</sub> kg<sup>-1</sup>, respectively [3, 16].

### Extraction of phenolic compounds (PC)

PCs in the EVOO were extracted according to the method of the International Olive Council (COI/T.20/DocNo29/ Rev.1, 2017) with a slight modifications. A 3 g of oil sample was weighed into a 12 mL tube. Then, 3 mL of methanol (80%), 1.5 mL of hexane and 0.5 mL of syringic acid (60 ppm) (internal standard (IS) were added to the tube. The mixture was vortexed for 30 s and



**Fig. 1** The location of the olive garden of Sari Ulak variety used for the EVOO

centrifuged at 5000 rpm and 10 °C for 5 min. The methanolic lower phase was transferred to another tube and the extraction was repeated two more times. After that, the lower phases were combined and washed twice with 3 mL hexane, and the hexane phase was removed from the top. The obtained phenolic extract was used in PC, TPC, TAC and ABTS analysis [17].

#### **Total phenolic content (TPC) and total antioxidant capacity (TAC) analysis**

TPC of the sample was determined using the Folin-Ciocalteu method as described by Çapanoğlu et al. [18].

The results were calculated using a calibration curve created with solutions prepared at different concentrations of the gallic acid standard and expressed as mg gallic acid equivalent per 100 g sample. Determination of TAC of sample was performed using the DPPH radical scavenging capacity and carried out according to method of Osei et al. [19], with some modifications. The results were expressed as mg trolox equivalent (TE) per 100 g of sample.

#### **ABTS radical scavenging activity**

ABTS Radical Scavenging Activity of the samples was determined according to the method used by Schlesier et al. [20], and expressed as mg trolox equivalents (TE) per 100 g sample.

#### **Determination of fatty acid (FA) composition by GC-FID**

Approximately 100 mg of olive oil sample was shaken well by adding 10 mL of hexane to it. To obtain FAMES,

0.5 mL of 2 M KOH dissolved in methanol was added to this mixture and then swirled for 20 s. The oil composition in the samples was analyzed using a gas chromatography flame ionization detector (GC-FID) system (Shimadzu QP2020, Shimadzu Corp., Japan) coupled with an Rtx-2330 capillary column (0.20  $\mu$ m, 60 m  $\times$  0.25 mm, Restek, Bad Homburg, Germany). After 2 h of dark soaking, 1  $\mu$ L of the solution was injected into the GC in split mode (1:100). The detector and injection port temperature was set at 250 °C and helium (at a flow rate of 1 mL/min) was used as the carrier gas. Peak designations and relative percentages of their fields were calculated using FAMES' mixing standards [3, 16].

#### **Determination of phenolic compounds by HPLC**

PC in samples were analyzed using a Water Alliance e2695 HPLC system (Waters, Milford, MA, USA) consisting of a photodiode array detector (PDA) (Waters 2996, Milford, MA, USA) and an inertSustain C18 column (5  $\mu$ m, 4.6  $\times$  250 mm, GL Sciences, Tokyo, Japan). The phenolic extract was filtered through a 0.45  $\mu$ m polyvinylidene fluoride (PVDF) syringe filter before injection into the HPLC system. The analysis conditions of HPLC were performed as described by Veneziani et al. with minor modifications. Results are expressed in mg kg<sup>-1</sup>. [4, 21].

#### **Determination of VC using SPME-GC-MS**

VCS in samples were determined by solid-phase microextraction (SPME) followed by the use of a gas chromatography-mass detector (GC-MS) (Shimadzu QP2020



brand, Kyoto, Japan) system connected to an autosampler (AOC 5000 Plus). The method was modified as described by Genovese et al. and Korkmaz et al. [3, 22].

### Sensory analysis of EVOO

A sensory panel of ten trained evaluators from the Central Laboratory of Artuklu University Mardin (Mardin, Türkiye) evaluated the samples in accordance with the Turkish Official Methods adapted to the IOC procedure. Positive characteristics (fruitiness, bitterness and burning) and defects (moldy, musty-smelling, wine-vinegar-like) were quantitatively determined by marking on the original profile sheet between 0 (no perception) and 10 (highest density) cm. The results were expressed as median values of the evaluators' perception scores [3, 16, 17].

### Determination of antimicrobial activity of EVOO

*Escherichia coli* ATCC 11229, *Klebsiella aerogenes* ATCC 13048, *Pseudomonas aeruginosa* ATCC 9027, *Klebsiella pneumoniae* ATCC 13883 were purchased from Microbiologics. Disk Diffusion method was applied to determine antimicrobial activity. (NCCLS 1997). Microorganisms taken from fresh culture were incubated in nutrient broth (NB) liquid medium at 37 °C until 0.5 Mc Farland ( $1.5 \times 10^8$  Kob/mL) turbidity occurred. Turbidity control was performed in a spectrophotometer at a wavelength of 625 nm with absorbances of 0.08–0.10. 100 µL of the cultured test microorganisms were taken and spread on nutrient agar solid medium. Then, 15 µL of each of the oils was impregnated on sterile discs placed in the transplanted petries. Inhibition zone diameters were measured for *Escherichia coli*, *Klebsiella aerogenes*, *Klebsiella pneumoniae*, *Pseudomonas aeruginosa*, bacteria after 24 h of incubation at 37 °C. Each test was performed in 3 repetitions at different times. Sulbactam/ampicillin (SAM) (20 µg) antibiotic discs were used as positive controls [23, 24].

### Network-based pharmacology

Predicted targets of Hydroxytyrosol, oleuropein, pinoselin and apigenin were obtained from a Swiss Target Prediction (<http://www.swisstargetprediction>). To identify the mutual targets of compounds we employed InteractiVenn online tool [25].

### Gene network analysis: gene enrichment analysis

We used ClusterProfiler, an ontology-based tool that offers three methods for gene classification and enrichment analyses: groupGO, richGO and richKEGG. ClusterProfiler provides a better understanding of the high-level functions of biological systems by comparing gene sets through biological term classification and

enrichment analyses. This package presents a method called groupGO to classify genes according to a specific level of the GO ontology and performs enrichment tests for GO terms and Kyoto Encyclopedia of Genes and Genomes (KEGG) paths based on hypergeometric distribution. Q values are also calculated so as not to keep the false discovery rate (FDR) high. In addition, ClusterProfiler offers a comparison function called CompareCluster, which automatically calculates the enriched functional categories of each set of genes, and various visualization methods [26, 27].

### Molecular modeling studies

#### Ligand system

Hydroxytyrosol, oleuropein, pinoselin and apigenin were retrieved from the PubChem (<https://pubchem.ncbi.nlm.nih.gov>) database in sdf format and converted to pdb format from the Open Babel GUI program (Table 1).

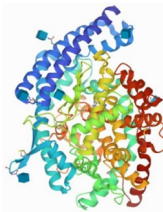

#### Protein system

A total of seven proteins that cause cardiovascular diseases were selected by literature review (Table 2). The crystal structures of these proteins are available in the Protein Data Bank ([www.rcsb.org](http://www.rcsb.org)). All polar hydrogens were added using the Discovery Studio 2020 modeling package to reduce the tension of the crystal structures and make the proteins usable in the Autodock simulation. The resulting structure was minimized in a vacuum environment; During minimization, the hydrogens were allowed to move while the heavy atoms were kept stable in their crystal coordinates. Proteins and ligands were prepared with the Autodocktools graphical user interface program; Gasteiger charges were calculated, and nonpolar hydrogens were combined with carbon atoms. The pdbqt files created for macromolecules were saved [28].

**Table 1** Major compounds found in EVOO and cardiovascular drugs for docking studies

No.	Molecule/drugs	Formula	Compound ID
1	Hydroxytyrosol	C <sub>8</sub> H <sub>10</sub> O <sub>3</sub>	82755
2	Oleuropein	C <sub>25</sub> H <sub>32</sub> O <sub>13</sub>	5281544
3	Pinoselin	C <sub>20</sub> H <sub>22</sub> O <sub>6</sub>	73399
4	Apigenin	C <sub>15</sub> H <sub>10</sub> O <sub>5</sub>	5280443
Cardiovascular (atherosclerosis/coronary artery diseases) drugs			
5	Losartan	C <sub>22</sub> H <sub>23</sub> ClN <sub>6</sub> O	3961
6	Lisinopril	C <sub>21</sub> H <sub>31</sub> N <sub>3</sub> O <sub>5</sub>	5362119

**Table 2** Targeted receptor proteins associated with Atherosclerosis along with structure

No.	Target proteins	Disease	PDB ID	Structure
1	Angiotensin converting enzyme	(Atherosclerosis/coronary artery diseases)	1O8A	
2	Human angiotensin receptor	(Atherosclerosis/coronary artery diseases)	4YAY	

### Molecular modeling

Data entry for modeling was created using the AutoDockTools (Autodock 4.2.6) program. In all models, a cube was formed consisting of squares with dimensions of  $80 \times 80 \times 80$  in the x, y, z directions. For energy calculations, an approach based on a distance of  $0.375 \text{ \AA}$  (about a quarter of the length of the carbon–carbon covalent bond) and a dielectric constant was adopted. The simulations, which were carried out using the Lamarckian genetic algorithm, were carried out with a study time of 10 times. Randomly placed fragments were simulated with 50 breakpoints, a maximum energy of  $2.5 \times 10^6$ , and a maximum occurrence of  $2.7 \times 10^4$ . The mutation rate was set at 2% and the genetic crossover rate was set at 80%. By combining the results with a mean root square deviation (RMSD) of less than  $0.5 \text{ \AA}$ , the structures with the best binding energy were determined as the final complex structures. Using the AutoDock Vina 1.1.2 and Discovery Studio 2020 programs, the optical spectra in EVOO and ligand–protein interactions were investigated for active regional localization studies [29, 30].

### ADME and ADMET

A new type of tool known as in silico ADME evaluation model has been developed to assist medical pharmacologists and chemists in pioneering discovery, development and optimization processes. SwissADME web server commonly used to predict the pharmacokinetics and drug-likeness properties of various substances (<http://www.swissadme.ch/>) [31]. Toxicity and metabolism estimation analysis was calculated using the

ADMETlab 2.0 website. <https://admetmesh.scbdd.com/service/evaluation/cal>. [32].

### Density functional theory analysis

Gaussian 09 software and GaussView 5.0 software were performed to carry out geometry optimization technique using DFT-based quantum chemistry simulations (B3LYP with a 6–311++G(d,p) [33]. The  $\Delta E$  value was calculated between LUMO and HOMO. The other calculated parameters were softness ( $s$ ), the dipole moment ( $\mu$ ) hardness ( $\eta$ ) and electronegativity ( $\chi$ ) [34–42]:

$$\Delta = E_{LUMO} - E_{HOMO}, \quad (1)$$

$$A = -E_{LUMO}, \quad (2)$$

$$I = -E_{HOMO}, \quad (3)$$

$$\eta = \frac{1}{2}(I - A), \quad (4)$$

$$s = \frac{1}{\eta}, \quad (5)$$

$$\chi = \frac{1}{2}(I + A). \quad (6)$$

The obtained identifiers for quantum compounds were shown in Table 16. It was discovered that this cholesterol had an energy gap of 3.187 eV, a  $E_{LUMO}$  of  $-0.607 \text{ eV}$  and a  $E_{HOMO}$  of  $-3.794 \text{ eV}$ . It's been proven that cholesterol has potent adsorption properties. Because of this, the cholesterol molecule is a good option for a chelating agent.

The molecule's computed quantum values for hardness electronegativity, and softness were 2.200 eV, 0.628 eV<sup>-1</sup>, and 1.594 eV, respectively. The  $E_{\text{HOMO}}$  and  $E_{\text{LUMO}}$  indicate the electron-giving and receiving abilities of molecules. As a result, a molecule's adsorption strength rises with a lower  $\Delta E$  value and its stability increases with a bigger molecular energy gap. The strength of the dipole moment (1.9001 D), which can change the dielectric properties of the double electric layer, increases the probability of cholesterol sticking. Because of its large dipole moment, cholesterol functions as a ligand for biological processes. The most common use for it is to calculate the electronegativity ( $\chi$ ) of compounds that gain or lose electrons. Electron attraction gets easier when a molecule's electronegativity increases. Greater global hardness ( $\eta$ ) was suggested to make charge transfer between molecules more difficult.

## Results and discussion

In this study, PC, VC, FA, TAC, ABTS analyzes of an EVOO obtained from a Turkish olive variety and ADMET, DFT, Molecular Docking and Gene network analysis of important molecules detected in EVOO were evaluated with computer-based programs. In addition, FFA, PV, K232 and K270 parameters were considered in the quality classification of EVOO. PV, K232, K270 are indicators for determining the level of oxidation in lipids, while FFA is considered a measure of enzymatic hydrolysis of lipids. Quality parameters are also affected by the degree of maturity of the olive, the extraction conditions used in oil production and the olive variety [3, 43, 44] The FFA, PV, K232 and K270 values of our study were 0.76 ± 0.02%, 17.61 ± 2.10 meq O<sub>2</sub>·kg<sup>-1</sup>, 1.24 ± 0.03, 0.176 ± 0.05, respectively. As shown in Table 3, FFA, PV, K232 and K270 values were among the recommended values [43]. When the quality parameters of our study were examined, the recorded values were consistent with the findings of previous studies [45, 46]. These parameters show that the oil meets quality standards and is high quality EVOO. High FFA values suggest that the oil has degraded or that the processing process has not attained a sufficient level of quality. Conversely, the FFA value of our study is low, suggesting that the oil is of high quality. A high peroxide value, K232 and K270 indicate that

**Table 3** Legal quality parameters in the EVOO of Sari Ulak Olives

Parameter	Mean ± SD
FFA (% Oleic acid)	0.76 ± 0.02
PV (meq O <sub>2</sub> ·kg <sup>-1</sup> )	17.61 ± 2.10
K232	1.24 ± 0.03
K270	0.176 ± 0.05

For EVOO; FFA (% oleic acid): Recommended ≤ 0.8; PV (meq O<sub>2</sub> kg<sup>-1</sup>): Recommended ≤ 20 K232: Recommended ≤ 2.50; K270: Recommended ≤ 0.22

the oil has progressed in the oxidation process and its quality has decreased. If the FFA value is low, it can be interpreted that the oil is protected from enzymatic degradation, the PV value is within the recommended limits, the oxidation level of the oil is acceptable, and the K232 and K270 values are low, the oil is fresh and the oxidation level is low.

When the fatty acid findings of our study were examined, oleic acid (71.85 ± 3.6), palmitic acid (11.70 ± 1.9), Linoleic Acid (9.00 ± 1.4), Stearic acid (3.01 ± 0.8), Palmitoleic Acid (0.73 ± 0.10), α-Linolenic acid (0.58 ± 0.009), Palmitoleic Acid (0.73 ± 0.10), Heptadecanoic acid (0.152 ± 0.07), Cis-10-Heptadecanoic acid (0.23 ± 0.08), Arachidic Acid (0.45 ± 0.8), 11-Eicosenoic acid (0.27 ± 0.06), Behenic Acid (0.11 ± 0.05), Tricosanoic acid (1.18 ± 0.1), Palmitoleic Acid (0.731 ± 0.09), PUFAs (9.58 ± 1.49), MUFAs (73.81 ± 3.93) were recorded (Table 4). In the literature, EVOO major component content was Oleic acid (63.1–79.7%), Palmitic acid value (9.4–19.5%), Linoleic Acid (6.6–14.8%), Stearic acid (1.4–3.0%), Palmitoleic Acid (0.6–3.2%), α-Linolenic acid (0.46–0.69%), PUFAs (7.0–15.5%), MUFAs (65.2–80.8%). The values are examined, all of the results we obtained fall within the expected literature range, when the olive oil obtained from Sariulak olives is evaluated in general, it possesses

**Table 4** Fatty acid profile (%) of EVOO obtained from Sari Ulak Olives

Oleic acid (C18:1)	71.85 ± 3.6
Palmitic acid (C16:0)	11.70 ± 1.9
Linoleic acid (C18:2)	9.00 ± 1.4
Stearic acid (C18:0)	3.01 ± 0.8
Alpha-linolenic acid (C18:3)	0.58 ± 0.09
Palmitoleic acid (C16:1)	0.73 ± 0.10
Heptadecanoic acid (C17:0)	0.152 ± 0.07
Cis-10-heptadecanoic acid (C17:1)	0.23 ± 0.08
Arachidic acid (C20:0)	0.45 ± 0.8
11-eicosenoic acid (C20:1)	0.27 ± 0.06
Behenic acid (C22:0)	0.11 ± 0.05
Tricosanoic acid (C23:0)	1.18 ± 0.1
Palmitoleic acid (C16:1)	0.731 ± 0.09
SFAs	16.60 ± 3.72
PUFAs	9.58 ± 1.49
MUFAs	73.81 ± 3.93
MUFAs/PUFAs	7.70 ± 2.6

For EVOO: Palmitic acid: 7.5 to 20.0; Palmitoleic acid: 0.3 to 3.5; Heptadecanoic: ≤ 0.3; Heptadecenoic acid: ≤ 0.3; Stearic acid: 0.5 to 5.0; Oleic acid: 55.0 to 83.0; Linoleic acid: 3.5 to 21.0. Arachidic Acid: Recommended ≤ 0.6; Behenic Acid: Recommended ≤ 1.0; Linolenic acid: Recommended ≤ 1.0; Results are expressed as Mean ± SD (standard deviation) (n = 3)

SFA saturated fatty acids, PUFA Polyunsaturated fatty acids, MUFAs Monounsaturated fatty acids

practically all of the legal quality characteristics and fatty acid profile of EVOO [2, 47, 48]. Oleic Acid and MUFA levels indicate that olive oil has a healthy fatty acid profile and meets quality standards in addition; levels of saturated fatty acids such as Palmitic Acid, Stearic Acid indicate that olive oil has a balanced fatty acid profile and is within quality limitations. Along with EVOO's rich and complex chemical profile, which includes more than 200 compounds, it is widely appreciated for its high nutritional value and largely proven nutritional properties. In particular, the Oleic acid forms MUFAs are the primary constituents of EVOO [48, 49]. Examining the main chemicals of EVOO in the present investigation reveals the results are largely consistent with previous research [44]. EVOO polyphenols have the ability to directly clean free radicals and break radical chains, as well as increase enzymatic endogenous antioxidant defense [50]. In this study, DPPH and ABTS radical scavenging activity values were converted to IC50. While the DPPH value was (IC50: 413.5 ± 217), the ABTS value was (IC50: 211.8 ± 16.2) (Table 5). The results suggest that EVOO has good free radical scavenging properties and high radical chain breaking capacity. The consumption of EVOO, which is the typical source of lipids in the cuisine of Mediterranean countries and especially one of the important representatives of the Mediterranean diet, is associated with a reduced risk of various chronic diseases such as diabetes, hypertension, obesity, cancer diseases and cardiovascular diseases (CVD) [51–53]. The burden of atherosclerotic cardiovascular illnesses, responsible for the majority of fatalities globally and have emerged as a major issue, must be reduced. It is specifically associated with the rise in atherosclerotic risk factors, which are linked to developing and advancement of cardiovascular disorders. Although risk factors were previously under control in many high-income countries, this disease, which is becoming an issue in low-income countries, is gradually losing ground in prevention even in high-income countries [54, 55]. By 2030, the direct cost of CVD treatment in the U.S. is projected to reach one trillion U.S. dollars. However, a healthy life will significantly reduce the burden and complications of atherosclerosis [56, 57].

Atherosclerosis begins with lipid deposits in the arterial intima, developing into a chronic inflammatory disease associated with myocardial infarction and stroke

**Table 5** DPPH and ABTS activity of EVOO

	Mean ± SD
DPPH (IC50)	413.5 ± 217
ABTS (IC50)	211.8 ± 16.2

Results are expressed as mean ± SD (standard deviation) (n = 3)

[54, 58]. This process involves the buildup of LDL-cholesterol and the activation of endothelial cells, which promotes inflammation [59]. EVOO supports the reduction of atherosclerotic risk through its anti-inflammatory, antioxidant, and vasodilatory effects [60]. Extensive evidence highlights the cardiovascular benefits of EVOO, extending beyond cholesterol reduction to include a variety of mechanisms. Its high nutritional value is due to a complex profile of over 200 compounds, with key contributions from oleic acid and polyphenols that are instrumental in preventing cardiovascular diseases [49, 61]. Notable phenolic components in EVOO include hydroxytyrosol, tyrosol, oleuropein, and a variety of phenolic acids, flavones, and lignans [62]. The examination of phenolic compounds demonstrated that, Hydroxytyrosol (2.33 ± 0.1 mg kg<sup>-1</sup>), Oleuropein (0.357 ± 0.01 mg kg<sup>-1</sup>), Pinoreosinol (0.115 ± 0.05 mg kg<sup>-1</sup>), Apigenin (0.23 ± 0.08 mg kg<sup>-1</sup>), Tyrosol (0.106 ± 0.04 mg kg<sup>-1</sup>), Vanillic acid (0.059 ± 0.010 mg kg<sup>-1</sup>), p-Qumaric acid (0.045 ± 0.008 mg kg<sup>-1</sup>), t-Ferulic acid (0.080 ± 0.009 mg kg<sup>-1</sup>), Caffeic acid (0.059 ± 0.007 mg kg<sup>-1</sup>), Total Phenolic Content (92.75 ± 5.9 mg GAE·kg<sup>-1</sup>) (Table 6). According to many studies, these effects in EVOO are largely due to the main secoiridoid derivatives such as oleuropein, oleocanthal, and oleacein. Additionally, simple phenols like hydroxytyrosol and tyrosol have been linked to a wide range of health-promoting effects, including antioxidant, anti-inflammatory, cardioprotective, neuroprotective, anticancer, antidiabetic, anti-obesity, antisteatotic, antimicrobial, etc. [63–65]. It is a monoterpene derivative of cyclopentane and consists of oleuropein, aglycon and glycoside, which has a bitter taste [66]. Oleuropein, a hydroxytyrosol ester containing an oleosidic skeleton and a carbohydrate group, has a beneficial effect on various aspects of cardiovascular disease through its vasodilator, anti-platelet aggregation, anti-inflammatory, anticancer,

**Table 6** Phenolic compounds (mg kg<sup>-1</sup>) of EVOO obtained from Sari Ulak Olives

Phenolic compound	Mean ± Std
Hydroxytyrosol	2.33 ± 0.11
Oleuropein	0.357 ± 0.01
Pinoreosinol	0.115 ± 0.05
Apigenin	0.23 ± 0.08
Tyrosol	0.106 ± 0.04
Vanillic acid	0.059 ± 0.010
p-Qumaric acid	0.045 ± 0.008
t-Ferulic acid	0.080 ± 0.009
Caffeic acid	0.059 ± 0.007
Total phenolic content (mg GAE·kg <sup>-1</sup> )	92.75 ± 5.9



and antioxidant properties [67, 68]. High amounts of tyrosol and hydroxytyrosol, the main phenolic compounds found in EVOOs, are found in the earliest harvest sample, while tyrosol and hydroxytyrosol concentrations decrease with increasing olive ripeness [69]. Hydroxytyrosol's potential in preventing and reducing cardiovascular risk factors has shown that, especially at higher doses in both in vitro and in vivo studies, it positively influences lipid profiles, plaque formation, and inflammatory processes following treatment [70]. Tyrosol is protective against cardiovascular diseases, as Tyrosol is effective in maintaining cellular antioxidant defenses through intracellular accumulation despite its weak antioxidant activity, which is in favor of olive oil consumption [71]. Apigenin prevents cardiovascular diseases through anti-apoptotic and antioxidant mechanisms in cardiomyocytes and vascular endothelial cells [72].

VC profile of EVOOs is responsible for their odor and has a key role in their sensory quality [73]. VC responsible for the characteristic EVOO aroma are formed generally by enzymatic and chemical oxidation during processing [74]. The composition of (VC) in EVOO of Sarı ulak olive are given in Table 7. A total of 40 volatile compounds were identified in the sample, including 6 terpenoids, 7 aldehydes, 7 alcohols, 5 esters, 2 ketones, 5 alkanes, 3 alkenes and 5 miscellaneous. Many of these compounds have also been reported from olive oil in several previous studies [3, 74]. The both number and content of VC in olive oils depends mainly on the variety as well as growing, processing and storage conditions [75]. Compounds C6 (hexanal, 1-hexanol, 3-(Z)-hexenol, and 2-(E)-hexenol) and C5 (1-penten-3-ol, 2-(Z)-pentenol) which are responsible for the typical aroma of the oil, were also detected in the EVOO sample in this study. These molecules are generated from linoleic and  $\alpha$ -linolenic acids via the lipoxygenase pathway and contribute to the pleasant odor of olive oil. Previous research has also identified these chemicals in EVOOs [76, 77]. However, as an interesting finding, (E)-2-hexenal (almond, green), one of the compounds found in most olive oils in previous studies and responsible for the characteristic olive oil aroma, was not detected in EVOO from Sarı Ulak olive in this study. On the other hand, estragole (38.94%), 7-hydroxyheptene-1 (10.48%) and 3-methoxycinnamaldehyde (12.98%) were quantitatively identified as the major compounds in the sample. To our knowledge, estragole and 7-hydroxyheptene-1 have not been reported in any olive oil before. The abundant presence of these compounds can be attributed to the characteristics of the olive variety. Terpenoid compounds 1,8-cineole,  $\delta$ -carene, (E)-phytol and farnesene, which contribute to the positive aroma of olive oil, were also found in the sample. These findings imply that the chemical components of this olive, and hence

the characteristic aroma of olive oil, might change significantly depending on the olive variety, growing conditions, and processing procedures. Nevertheless, some compounds that cause aroma defects, such as ethanol (winey), 2-methylbutanol (fusty) and (E)-2-heptenal (rancid), were also found in the EVOO sample. Among these, the first two generated due to microbial activity, while the last one occurs based on lipid autoxidation [78].

In order to provide the best possible information to the consumer thanks to sensory analyzes other than chemical and physical analysis, the oils are usually labeled as Dense/robust, medium or sensitive/light according to their properties. In the method used, fruitiness, bitterness and pungency (intensity/positive/positive) and Moldy, winey-vinegary (imperfect/negative) quantitative density are given a value between 0 (no perception) and 10 (highest intensity). (Median, Sturdy > 6; when the median of the middle feature is between 3 and 6; when the median of the feature is Precision < less than 3.0). [79, 80]. In sensory analysis, EVOO needs to show a fruity note higher than 0 and, more importantly, a median of zero defects [81]. It was evaluated by a trained sensory panel/tasters consisting of ten evaluators from the Central Research Laboratory of Mardin Artuklu University (Mardin, Türkiye) in tasting sessions of four samples at approximately 15-min intervals, according to the Turkish Official Methods (2014), adapted from the IOC (2018) procedure. The obtained data was entered into the computer [3, 16, 80] When the sensory analysis results were examined, it had positive characteristics such as Fruitiness ( $3.5 \pm 0.49$ ), Bitterness ( $3.8 \pm 0.28$ ), Pungency ( $3.25 \pm 0.63$ ). When the negative traits were examined, the quantitative intensity of Winey-vinegary, Fusty, Musty was 0 (Table 8). Examples of EVOO; It did not show antimicrobial effects in *E. coli*, *K. pneumoniae*, *K. aerogenes* bacteria. On *P. aeruginosa*, it produced an inhibition diameter of 8.0. Compared to 20  $\mu$ g sulbactam/ampicillin antibiotic, 15  $\mu$ L of olive oil showed an inhibition effect of 69.57% (Table 9; Fig. 2). The fact that it does not show antimicrobial effects in bacteria such as *E. coli*, *K. pneumoniae* and *K. aerogenes* indicates that olive oil is ineffective against these bacteria, while this indicates that olive oil does not have an overall antimicrobial activity against all bacterial pathogens. On the contrary, it can be said that this olive oil provides a noticeable inhibition effect on *P. aeruginosa*, but its effect is limited. It can be interpreted that olive oil provides a similar effect on *P. aeruginosa* as antibiotics, but the effect may be less potent.

Gene network analysis helps us understand cellular signal transduction and regulatory processes in a systematic way by identifying biological interactions between genes. It describes how a group of genes interact with each other to form a functional module, and how



**Table 7** Relative concentration (% area) of volatile compounds in EVOO of Sari Ulak Olives

No.	Compound <sup>a</sup>	RI <sup>b</sup>	Relative percentage (%) <sup>c</sup>
<i>Terpenoids</i>			3.38
1	1,8-Cineole	1225	0.33
2	δ-Carene	1267	0.43
3	(E)-4,8-Dimethyl-1,3,7-nonatriene	1318	0.33
4	Farnesene	1754	0.54
5	(E)-Phytol	1972	1.21
6	Rosifoliol	2243	0.53
<i>Aldehydes</i>			22.13
7	Pentanal	1027	0.33
8	Hexanal	1115	7.24
9	(E)-2-Pentenal	1155	0.29
10	(E)-2-Heptenal	1338	0.34
11	Nonanal	1403	0.41
12	(E,E)-2,4-Heptadienal	1474	0.54
13	3-Methoxycinnamaldehyde	1790	12.98
<i>Alcohols</i>			6.80
14	Ethanol	989	0.71
15	1-Penten-3-ol	1181	0.67
16	2-Methylbutanol	1223	0.34
17	2-(Z)-pentenol	1329	0.37
18	1-Hexanol	1360	1.63
19	3-(Z)-Hexenol	1390	2.19
20	2-(E)-Hexenol	1411	0.88
<i>Esters</i>			3.81
21	Methyl acetate	907	0.34
22	Ethyl Acetate	949	0.63
23	Hexyl acetate	1289	0.49
24	(4E)-4-Hexenyl acetate	1333	1.74
25	Methyl cinnamate	2095	0.60
<i>Ketones</i>			1.69
26	3-Pentanone	1026	1.28
27	6-Methyl-5-Hepten-2-One	1351	0.41
<i>Alkanes</i>			3.15
28	2,4-Dimethylhexane	868	1.17
29	1-Methoxyhexane	1003	0.70
30	2,2,4,6,6-Pentamethylheptane	1009	0.28
31	Cyclohexane	1273	0.28
32	Hexatriacontane	2189	0.73
<i>Alkenes</i>			13.41
33	Z-1-Methoxy-3-hexene	1048	0.27
34	7-Hydroxyheptene-1	1238	10.48
35	1-Tetradecene	1255	2.65
<i>Miscellaneous</i>			45.63
36	3-Ethyl-1,5-octadiene	1050	0.60
37	Estragole	1684	38.94
38	1,5,9,9-Tetramethyl-1,4,7-cycloundecatriene	1784	0.61
39	Anethole	1842	1.88
40	Methyleugenol	2018	3.61

**Table 7** (continued)

<sup>a</sup> Compounds were identified by comparing their mass spectra with those in MS libraries (NIST11 and Wiley9)

<sup>b</sup> RI, Retention indices (Calculated on DB-HeavyWax capillary column)

<sup>c</sup> %, The ratio of the peak area of each compound to the total area of all peaks in the chromatogram obtained from GC-MS (results were calculated as the average of three replicates)

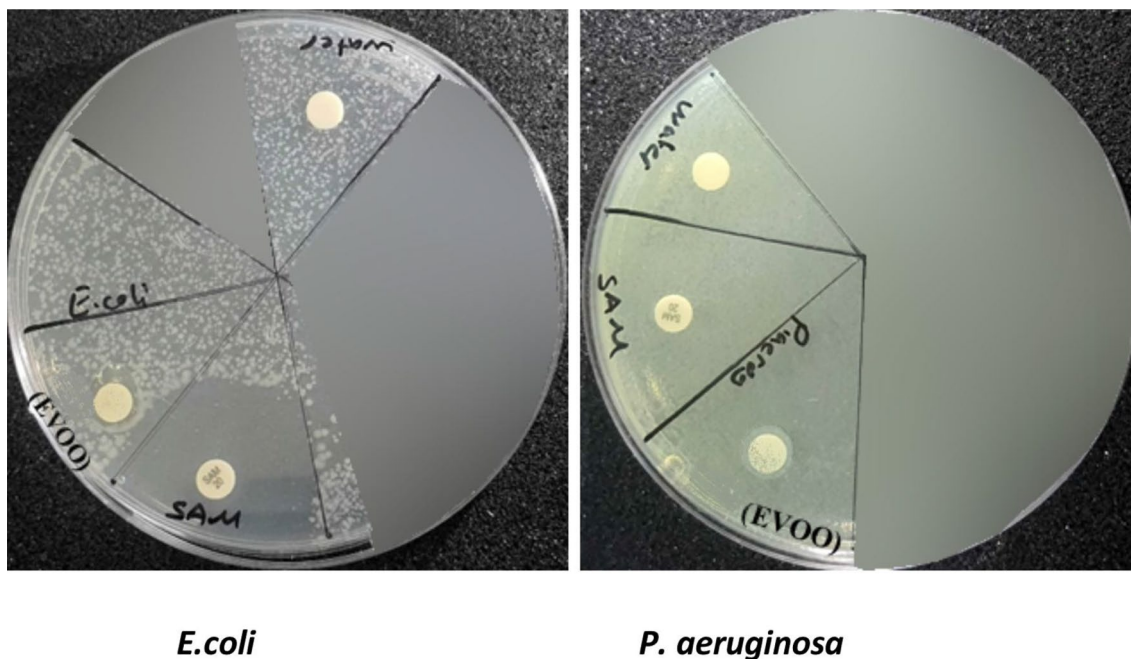
**Table 8** Sensory properties of EVOO obtained from Sari Ulak Olives

Scores of sensory attributes of EVOO obtained from Sari Ulak olive	Mean ± Std
Fruitiness	3.5 ± 0.49
Bitterness	3.8 ± 0.28
Pungency	3.25 ± 0.63
Winey-vinegary	–
Fusty	–
Musty	–

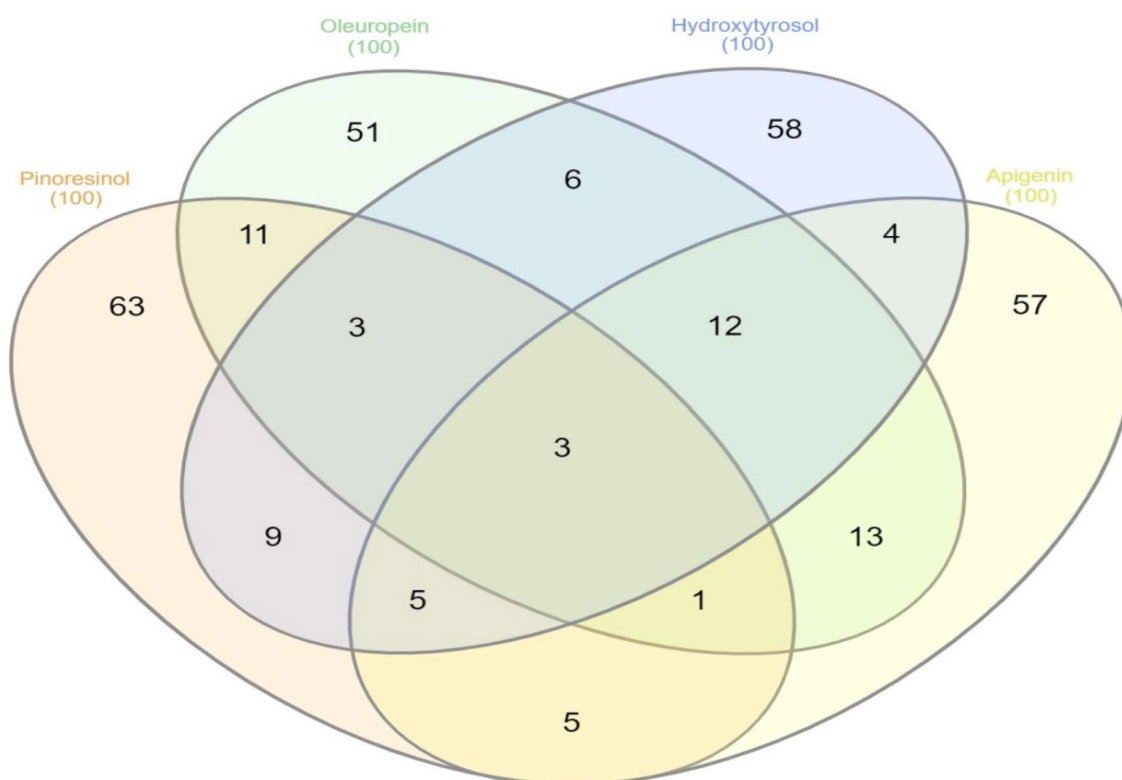
**Table 9** Antimicrobial analysis results (inhibitions zone diameters ± SD)

	<i>E.coli</i>	<i>K. pneumoniae</i>	<i>P. aeruginosa</i>	<i>K. aerogenes</i>
SAM			11.5 ± 0.7	
EVOO	–	–	8.0 ± 0.0	–

different gene modules are linked to each other [82]. Target gene predictions of bioactive important compounds in EVOO were extracted, and common gene associations of pinorelinol, apigenin, hydroxytyrosol, and oleuropein were found to be more frequent (Fig. 3). It implies that these compounds can affect similar biological pathways and exert a joint effect on these pathways. The frequent occurrence of co-gene associations may suggest that these compounds are involved in the same or similar cellular processes, for example, that they may exhibit joint effects on antioxidant defense, inflammation modulation, or cellular signaling pathways. With these common genes, a relationship was established between lipids and atherosclerosis in KEGG enrichment analysis. The Swiss Target prediction web tool was used to predict the target genes for each of EVOO’s major molecules. The Venn diagram (Fig. 3) is depicted to analyze the genes shared for each of the major molecules of EVOO. CA3, TYR, CA14, CA9, ADORA1, ADORA2A, CA1, CA6, CA2, CA12, CA7, and PARP1 have been shown to frequently



**Fig. 2** Antimicrobial demonstration of EVOO obtained from Sari Ulak Olives



**Fig. 3** Venn diagram of the intersection between targets of each of Hydroxytyrosol, oleuropein, pinosresinol and apigenin target genes

be shared between apigenin, hydroxytyrosol, and oleuropein. The KEGG enrichment analysis conducted with these 12 genes revealed the relationships between apigenin, hydroxytyrosol, and oleuropein—compounds targeted in our study—and lipids and atherosclerosis (Figs. 3, 4, 5). These data imply that the main compounds of EVOO, such as apigenin, hydroxytyrosol, and oleuropein, could potentially exert protective or regulatory effects on lipid metabolism and atherosclerosis through these genes. It also supports that these components may have beneficial effects on cardiovascular health, especially in processes such as lipid metabolism and regulation of atherosclerosis.

As a result of gene enrichment analysis, pinosresinol, apigenin, hydroxytyrosol and oleuropein were inserted into lipid and atherosclerosis-targeting protein structures (PDB ID: 1O8A and 4YAY) by molecular docking method. In the comparison of pinosresinol, apigenin, hydroxytyrosol and oleuropein compounds, lisinopril for 1O8A and losartan for 4YAY were used as the standard. When molecular docking for 1O8A was examined, apigenin (−8.5 kcal/mol) had a better binding score than pinosresinol and oleuropein lisinopril. Oleuropein showed good binding score in 1O8A protein structure. When molecular docking for YAY was examined,

Hydroxytyrosol (− 5.9 kcal/mol), Oleuropein (− 7.8 kcal/mol), Apigenin (− 8.2 kcal/mol) had lower binding scores than Losartan. Pinosresinol (− 8.5 kcal/mol) showed a higher binding score than other molecules in the 4YAY protein structure and equal binding score with Losartan (Fig. 6 and Table 10). The hydrophobic and hydrogen bond interactions of apigenin, hydroxytyrosol, oleuropein, Pinosresinol and CVD inhibitors, which are important in drug targets, are given in Table 11 and Fig. 7. Angiotensin converting enzyme (ACE, PDB ID:1O8A) is important component of renin–angiotensin–aldosterone system (RAAS), which converts angiotensin I to angiotensin II and is expressed in many different cell types [83]. Changes in ACE function have been associated with CVDs such as CAD, HF, and hypertension in previous studies [84]. Angiotensin II Type I Receptor (AT1R, PDB ID: 4YAY), which involved in cellular proliferation, apoptosis, fibrosis and inflammation is a member of the G protein-coupled receptor family that regulates RAAS signal transduction [85–87]. AT1R causes atherosclerosis through Angiotensin II-led inflammation in pathological conditions, and AT1R blockers are essential components of the treatment of coronary atherosclerosis [58, 88–91].

Physicochemical properties and predictions about ADME are based on drug similarity rules. In our study,

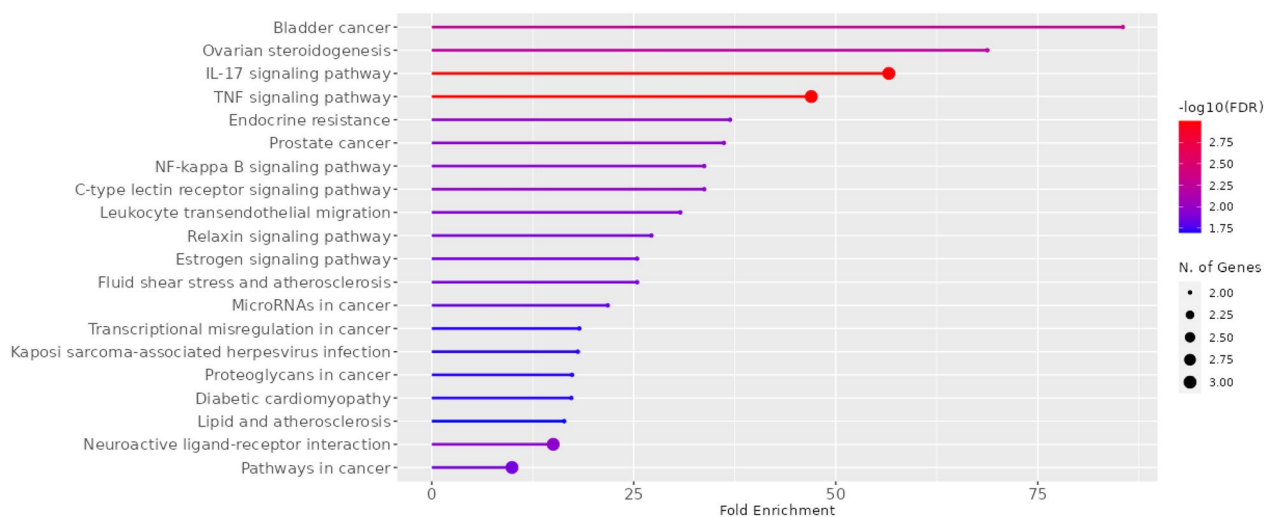
Names	total	elements
Apigenin Hydroxytyrosol Oleuropein Pinoresinol	3	MMP13 CDK2 TOP1
Hydroxytyrosol Oleuropein Pinoresinol	3	CHEK1 PDE5A PNP
Apigenin Oleuropein Pinoresinol	1	ABCB1
Apigenin Hydroxytyrosol Pinoresinol	5	ALOX5 CXCR1 ESR2 GSK3B PIM1
Apigenin Hydroxytyrosol Oleuropein	12	CA3 TYR CA14 CA9 ADORA1 ADORA2A CA1 CA6 CA2 CA12 CA7 PARP1
Oleuropein Pinoresinol	11	MMP7 MMP8 MAPK1 SLC5A2 PIK3CA PRSS3 F9 IRAK4 MMP1 SLC5A4 PRSS1
Hydroxytyrosol Pinoresinol	9	JAK1 JAK2 ALOX5AP HDAC1 LRRK2 PLA2G7 ALPL HDAC6 TDP1
Apigenin Pinoresinol	5	ALOX12 TTR PYGL ESR1 CDK1
Hydroxytyrosol Oleuropein	6	CDK2 CCNA1 CCNA2 ALDH2 TYMS VEGFA EPHX2 HSP90AA1
Apigenin Oleuropein	13	MMP2 PLG CYP19A1 TNKS2 MMP3 CA4 PTGS2 TNKS ST6GAL1 SYK ADORA3 DRD4 MMP9
Apigenin Hydroxytyrosol	4	AURKB ABCG2 EGFR ACHE
Pinoresinol	63	DPP8 ACE PTGER3 TLR4 TARS MTOR SLC6A2 NR3C2 BRD4 STS PTAFR GRIN2A GRIN1 SLC6A4 CNR2 PIK3C2B CCR1 FCER2 MAPKAPK2 PCNA HDAC4 EDNRB GABRA5 DPP7 NR1H2 NR1H3 LYPLA1 PIK3CG KMO DPP4 ERBB2 PRF1 SHBG MAP4K4 BDKRB1 LYPLA2 CTSD PIK3C3 PIK3CD CXCR2 HDAC8 QPCT ERN1 CSF1R BMP1 HDAC2 MAP3K12 SOAT1 FFAR1 TDP2 FBP1 MCL1 HIF1A DUT ADA EIF2AK3 SCN9A SCN5A MAPK9 WEE1 CNR1 DHFR SOAT2 OPRM1
Oleuropein	51	HLCS NADK SLC37A4 SLC28A3 CA13 TNF YARS MAP3K7 DRD2 CA5B ITGB1 ITGA4 ADAM17 FNTA FNTB SLC28A2 TACR2 PGF SLC5A1 IMPDH1 PRKACA HCAR2 LGALS4 MAP2K1 MARS CA5A LGALS1 TRPM2 IL2 AKR1C3 LGALS3 SRD5A1 ACE2 AGTR1 IGFBP3 HSPA5 ALB LGALS8 PTGS1 GBA F3 HRAS MME JUN ADK MGMT HSPA8 PRKCA NRAS SLC2A1 SLC29A1 ADORA2B GBA2
Hydroxytyrosol	58	KCNMA1 ILK IDO1 PDGFRA PDGFRB PDGFRB NOS2 FLT1 TLR9 YWHAG FGFR1 ALPG CDK9 CCNT1 PTK2B JAK3 MPI FADS1 CYP1A2 EGLN1 PDGFRA PDPK1 UPP1 XIAP PRKAB1 CES2 MIF MKNK1 MB GABRB3 GABRG2 GABRA5 ASF1A TMIGD3 PRKDC HDAC5 DAPK3 HDAC7 QDPR GSK3A PNMT DNM1 DCTPP1 CSNK1D GRM5 DBF4 CDC7 CHRNA4 CHRNB2 DAO FEN1 GABRA2 GABRB3 GABRG2 PRKD1 NAT1 ADAMTS5 CCNE1 CDK2 CSNK1A1 PLEC PLAA DBH PIM2 TUBB1 HDAC9 GPR84
Apigenin	57	XDH HSD17B1 HSD17B2 KDR CDK6 GLO1 CAMK2B LCK PTPRS CCNB3 CDK1 CCNB1 CCNB2 MET AXL AMY1A MPO AKR1B10 AKT1 PIK3R1 GRK6 CDK5R1 CDK5 F2 SLC22A12 TBXAS1 ARG1 NAE1 PLK1 HTR2C ABCC1 CD38 NOX4 FLT3 ALK MAOA PFKFB3 PTK2 BCHE IGF1R GPR35 ESRRA AVPR2 AR AKR1B1 MPG CSNK2A1 DAPK1 ALOX15 TERT NEK2 MMP12 CFTR APP CYP1B1 PKN1 SRC AHR CBR1 NEK6 KDM4E

**Fig. 4** Venn diagram of the intersection between targets of each of Hydroxytyrosol, oleuropein, pinoresinol and apigenin target genes list

Oleuropein failed to pass the rule with three violations ( $MW > 500$ ,  $NorO > 10$ ,  $NH_{OH} > 5$ ), Ghose ( $MW > 480$ ,  $WLOGP < -0.4$ ) with two violations, and Egan ( $TPSA > 131.6$ ) with one violation. Hydroxytyrosol only had a violation of the Ghose rule ( $MW < 160$ ). Hydroxytyrosol passed the full set of Lipinski, Veber, Egan. There were no violations of Apigenin and Pinoresinol. He completely passed all the rules. Hydroxytyrosol

has an H-bond acceptor value of 3, and H-bond acceptors value is 3, while Rotatable bonds value is 2. Oleuropein has an H-bond donor value of 6, and H-bond acceptors value is 13, and Rotatable bonds value is 11. Apigenin's H-bond acceptors value is 3, and H-bond acceptors value is 5, and Rotatable bonds value is 1. Pinoresinol H-bond donors have a value of 2, and H-bond acceptors value is 4, and Rotatable bonds value is 4. A radar





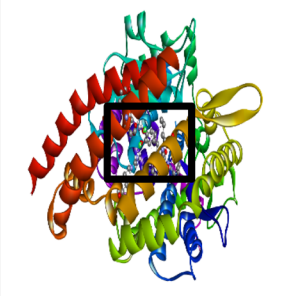
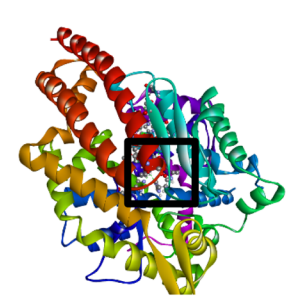
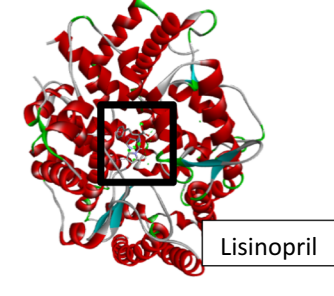


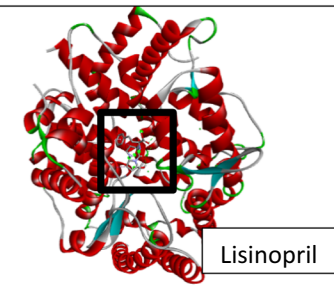
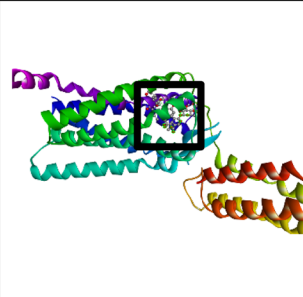
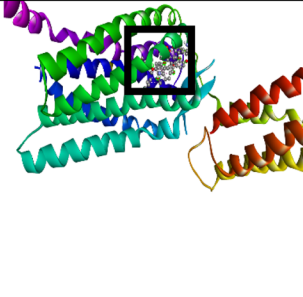

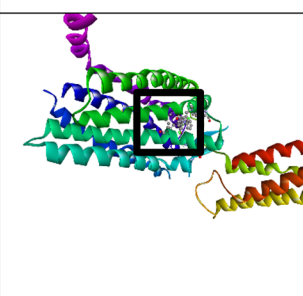
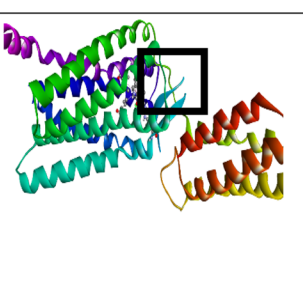
**Fig. 5** KEGG enrichment analysis of Hydroxytyrosol, oleuropein, pinosresinol and apigenin

map was created to evaluate and compare the molecules of Hydroxytyrosol, Apigenin, Oleuropein, Pinosresinol using six physicochemical properties such as size, lipophilicity, polarity, solubility, saturation and elasticity. The region shown in the diagram corresponds to the optimal range of values of each parameter. In the diagrams provided, Apigenin exhibited an optimal range (shown in pink area) for all criteria except Insatu (Saturation), while Oleuropein was outside the optimal range for Size, Polarity, and Flexibility. Hydroxytyrosol and Pinosresinol were within an optimal range for all criteria in the diagrams provided (Fig. 8). Hydroxytyrosol, Apigenin, Pinosresinol, Oleuropein showed Log Po/w (XLOGP3) values below 5; this suggests good permeability and absorption across the cell membrane. Furthermore, The solubility of a molecule is an important factor that plays a huge role in the absorption of the compound in the formulation process. Hydroxytyrosol, Apigenin, Pinosresinol exhibited 55% oral bioavailability. While this value was acceptable, Oleuropein exhibited a low value, i.e. 11% oral bioavailability (Table 12). In the light of these findings, it shows that Hydroxytyrosol, Apigenin and Pinosresinol are more advantageous in terms of pharmacokinetics and may be more suitable candidates in the drug development process. But Oleuropein's large size, low solubility, and bioavailability may make it pharmacologically disadvantageous. The lowest Synthetic accessibility value is Hydroxytyrosol, and the highest Synthetic accessibility value is the highest Oleuropein, the closer this value is to 1, the easier it can be synthesized, while the closer to 10, the more difficult it is to synthesize [31]. Log S (ESOL: Estimating Aqueous Solubility) is the in silico estimation of the aqueous solubility of molecules, including

the effect of the topological polar surface area. The Log S scale value ranges from  $-10$ . (insoluble),  $-6$  (poorly soluble),  $-4$  (soluble),  $-2$  (very soluble) and  $0$  (very soluble) [92, 93]. The TPSA value is expected to be between 20 and 130 Å<sup>2</sup>. The only Oleuropein ((201.67 Å<sup>2</sup>) molecule that did not fit this TPSA value range was [31].

Inhibition and induction of CYPs are among the main mechanisms that cause pharmacokinetic drug-drug interactions, and CYP1A2, CYP2C19, CYP3A4, CYP2C9 and CYP2D6 are important CYPs preferred especially in silico assays [94, 95]. Hydroxytyrosol and Oleuropein were not inhibitors for CYP1A2, CYP2C19, CYP2C9, CYP2D6 and CYP3A4. Apigenin and Pinosresinol were inhibitors for CYP2D6, CYP3A4. Apigenin alone was inhibitory for CYP1A (Table 13). The fact that Apigenin and Pinosresinol inhibit the enzymes CYP2D6 and CYP3A4 indicates that these compounds could potentially interact with other drugs. In addition, the fact that Apigenin is an inhibitor of CYP1A requires careful use, especially with drugs that this enzyme metabolizes. Hydroxytyrosol is synthetically a more readily accessible compound, has good aqueous solubility, and has a low risk of pharmacokinetic interactions. On the contrary, Oleuropein is synthetically harder, has low aqueous solubility, and limited bioavailability. Apigenin and Pinosresinol should be carefully evaluated for potential drug-drug interactions as they can inhibit some CYP enzymes. These findings provide important insights into how Apigenin and Pinosresinol should be addressed in the pharmaceutical development process.

Since the study of ADME pharmacokinetics (absorption, distribution, metabolism, excretion) is an important factor in the development of drugs, it saves drug

Target Protein	Hydroxytyrosol	Oleuropein	Cardiovascular Inhibitors
1O8A			 Lisinopril
Target Protein	Pinoresinol	Apigenin	Cardiovascular Inhibitors
1O8A			 Lisinopril
Target Protein	Hydroxytyrosol	Oleuropein	Cardiovascular Inhibitors
4YAY			 losartan
Target Protein	Pinoresinol	Apigenin	
			

**Fig. 6** Molecular Docking patterns of Hydroxytyrosol, oleuropein, pinoresinol, apigenin, cardiovascular inhibitors in target proteins structures

**Table 10** Docking score of Hydroxytyrosol, oleuropein, pinosresinol, apigenin, and cardiovascular inhibitors against their target protein receptors

Molecule	1O8A	4YAY
Hydroxytyrosol	− 6.0 kcal/mol	− 5.9 kcal/mol
Oleuropein	− 8.7 kcal/mol	− 7.8 kcal/mol
Pinosresinol	− 8.3 kcal/mol	− 8.5 kcal/mol
Apigenin	− 8.5 kcal/mol	− 8.2 kcal/mol
Inhibitors	− 7.0 kcal/mol	− 8.5 kcal/mol
	Lisinopril	Losartan

Docking score was expressed in kcal/mol

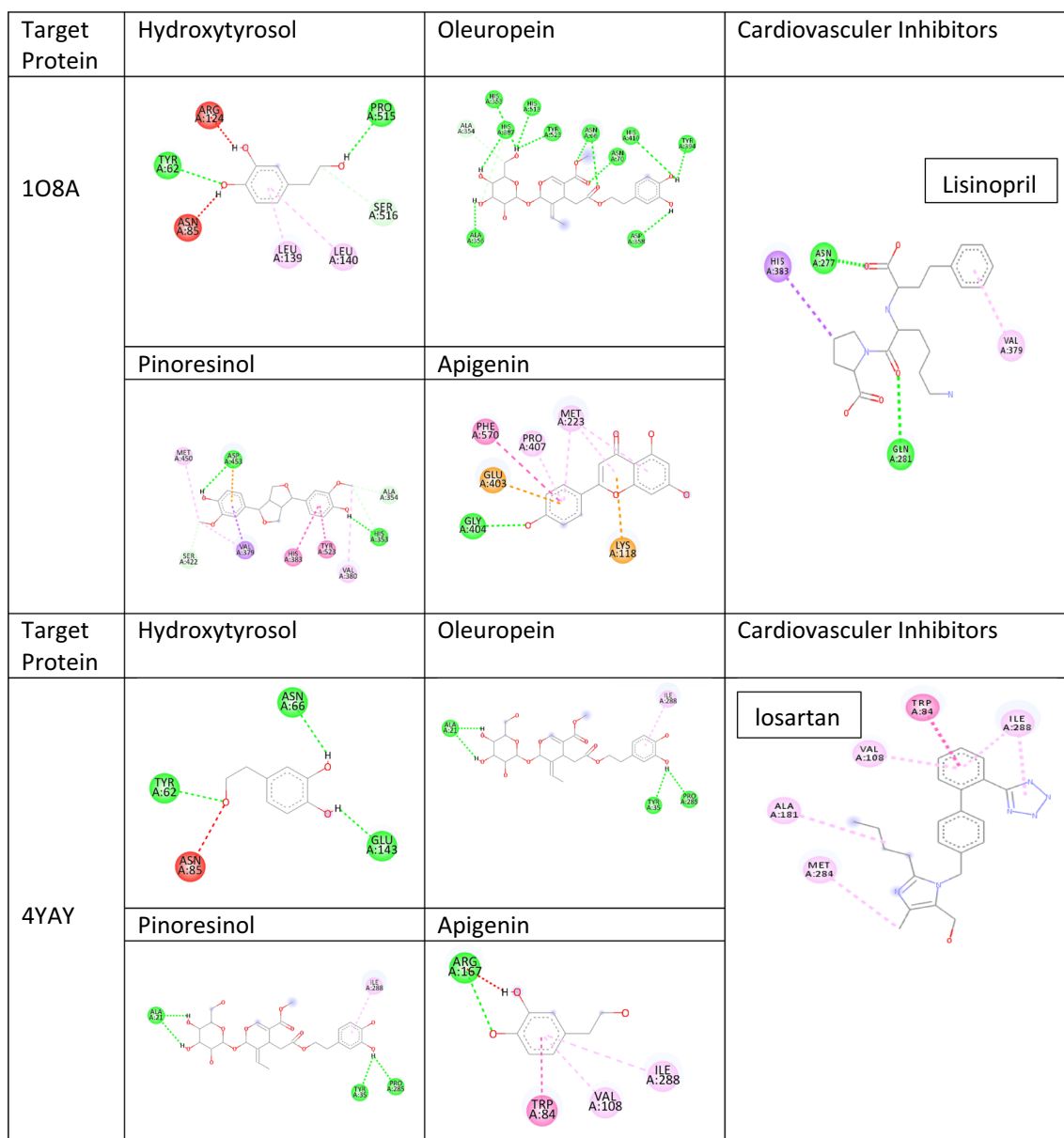
development time costs and supports experimental studies [96]. In our study, except for Oleuropein, Hydroxytyrosol, Apigenin, Pinosresinol were well absorbed because their gastrointestinal absorption (GI) was high. In addition, Pinosresinol appears to be able to cross the blood–brain barrier (Table 14). To evaluate the absorption property of Hydroxytyrosol, Oleuropein, Apigenin, Pinosresinol substrate or inhibitor (P-gpnh/P-gpsub), Caco-2-Permeability, human intestinal absorption (HIA) was estimated. 20% bioavailability (F20) and 30% bioavailability (F30) are as presented (Table 14). A positive value of F20 and F30 means that a compound is bioavailable up to 20% and 30% in the human body. The fact that the values are negative means that they cannot be used biologically. The F20 and F30 value of Hydroxytyrosol,

Apigenin are positive. Oleuropein F20 is low negative, while F30 value is high positive. When looking at pinosresinol, both F20 and F30 values show high negative properties. Negative means a low oral bioavailability. Caco-2 cells are used to analyze how a molecule penetrates it Caco-2 permeability Hydroxytyrosol (− 4.43 cm/s), Oleuropein (− 5.8 cm/s), Apigenin (− 4.84 cm/s), Pinosresinol (− 4.79 cm/s). The increase of high negative Caco-2 mainly means that it has the potential to provide their permeability (Table 14). Hydroxytyrosol has a low negative value, indicating that this compound can pass through the intestine relatively well, while Oleuropein has a more negative value than other compounds, which can be interpreted as having lower permeability.

Hydroxytyrosol, Oleuropein, Apigenin and Pinosresinol HIA data were categorically represented as 0 and 1. HIA values are Hydroxytyrosol (++), Oleuropein (+++), Apigenin (− −) and Pinosresinol (− −), F20 values are Hydroxytyrosol (+++), Oleuropein (−), Apigenin (+++) and Pinosresinol (−−), F30 values are Hydroxytyrosol (+++), Oleuropein (+++), Apigenin (+++) and Pinosresinol (− −). When the HIA values are examined, it can be interpreted that Hydroxytyrosol and Oleuropein have a good absorption potential in the intestines, while Apigenin and Pinosresinol have a low absorption potential in the intestine. Hydroxytyrosol and Apigenin F20 and F30 values are positive when examined. This means that compounds can bioavailable in the human body at a rate of 20% and 30%, meaning that these compounds have a

**Table 11** H-bond and hydrophobic interaction between high binding score compounds and receptor

Target Protein	Hydroxytyrosol H-bond	Hydroxytyrosol Hydrofobic	Oleuropein H-bond	Oleuropein Hydrofobic	Pinosresinol H-bond	Pinosresinol hydrofobic
1O8A	TYR62, PRO515, SER516	ASN85, ARG124, LEU139, LEU140	ASN66, ASN70, HIS353, ALA354, ALA356, ASP358, HIS387, TYR394, HIS410, HIS513	−	HIS353, ALA354, SER422, ASP453,	VAL379, VAL380, HIS383, MET450, TYR523
	Apigenin H-bond	Apigenin Hydrofobic			Cardiovasculer Inhibitors H-bond	Cardiovasculer Inhibitors Hydrofobic
	GLY404	LYS118, MET223, GLU403, PRO407, PHE570			ASN277, GLN281	HIS383, VAL379
Target Protein	Hydroxytyrosol H-bond	Hydroxytyrosol Hydrofobic	Oleuropein H-bond	Oleuropein Hydrofobic	Pinosresinol H-bond	Pinosresinol Hydrofobic
4YAY	TYR62, ASN66, GLU143	ASN85	ALA21, TYR35, PRO285	ILE288	ASP281	TRP84, TYR92, VAL108, ILE288
	Apigenin H-bond	Apigenin Hydrofobic			Cardiovasculer Inhibitors H-bond	Cardiovasculer Inhibitors Hydrofobic
					−	TRP84, VAL108, ALA181, MET284, ILE288

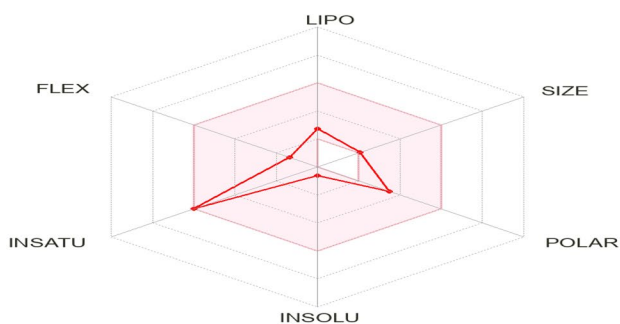
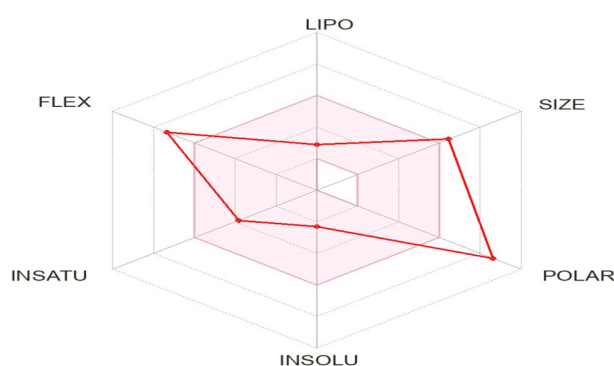
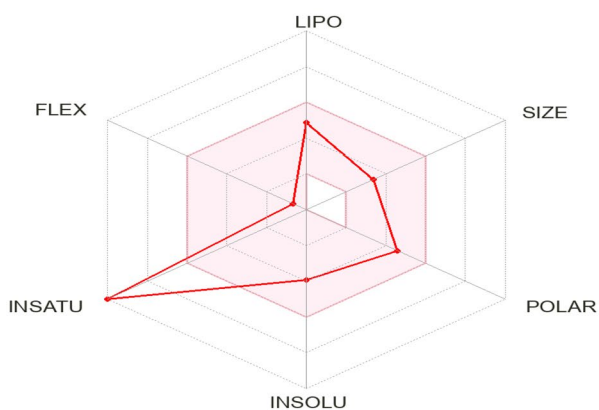
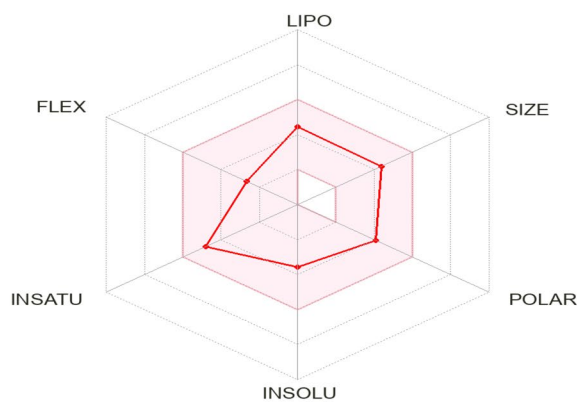


**Fig. 7** Discovery Studio structure showing interactions between Hydroxytyrosol, oleuropein, pinoresinol, apigenin, cardiovascular inhibitors and target proteins

good bioavailability potential when taken orally. However, the Oleuropein F20 value is low negative, which indicates that the 20% bioavailability is quite low, while the high positive F30 value means that the potential to reach 30% bioavailability is high. This suggests that the bioavailability of Oleuropein may increase depending on dose or intake conditions. When we looked at pinoresinol, both F20 and F30 values were found to be highly negative, which means that pinoresinol will have very low bioavailability after oral ingestion and cannot be bioused in the body. PPB states that the effectiveness of a drug

is related to how much it binds to proteins in the blood plasma. When the drug is less bound to proteins, it can pass or diffuse through cell membranes more effectively (Table 14) [97]. Since absorption and distribution affect each other, if the human body cannot easily absorb a drug, the distribution of the drug will also be poor [98]. The T1/2 half-life is defined as the time it takes for the plasma concentration of a drug to decrease by 50%. More than 30 min is considered a good half-life value. Hydroxytyrosol T1/2 value is 0.9, VD value is 1.12, Oleuropein T1/2 value is 0.83, VD value is 0.56, Apigenin T1/2 is



**A: Hydroxytyrosol****B: Oleuropein****C: Apigenin****D: Pinoreosinol**

**Fig. 8** Radar map of Hydroxytyrosol (A), Oleuropein (B), Apigenin (C), Pinoreosinol (D) molecules taken from Swissadme database (the pink area shows the optimal range for each property (lipophilicity: XLOGP3 between  $-0.7$  and  $+5.0$ , Size: MW between 150 and 500 g/mol, polarity: TPSA between 20 and 130 Å<sup>2</sup>, solubility: log S not higher than 6, Saturation: fraction of carbons in the sp<sup>3</sup> hybridization not less than 0.25, and Flexibility: no more than 9 rotatable bonds)

0.85, VD value is 0.510, Pinoreosinol T<sub>1/2</sub> value is 0.43, VD value is 1.052. A high VD value indicates that the drug is distributed more into tissue, while a low VD value indicates that the drug remains mostly in the plasma. In this case, we can say that Hydroxytyrosol and Pinoreosinol have a wider distribution in the body. Since the whole is under 3.0 h, the drugs have a low T<sub>1/2</sub>, which indicates that the drug is removed from the human body at a reasonable rate. T<sub>1/2</sub> depends on the rate constant (k), which is associated with VD and purge (CL). The CL values of Hydroxytyrosol, Oleuropein, Apigenin, Pinoreosinol are 17.2, 2.5, 7.02, 7.89, respectively. The lowest is Oleuropein, while the highest is Hydroxytyrosol [99, 100].

Below 5 mL/min/kg means that the renal clearance rate is low. These parameters are interconnected as the slower

the CL, the longer the T<sub>1/2</sub>. Only Oleuropein shows this property [98]. Oleuropein has the lowest CL value, indicating that this drug will stay in the body longer and be cleared more slowly. We can say that hydroxytyrosol has the highest clearance rate and hence is eliminated from the body the fastest. However, Oleuropein's low CL value and relatively long T<sub>1/2</sub> value suggest that this drug may stay in the body for a longer period of time and therefore exert longer-lasting effects. In particular, Oleuropein's low CL and relatively long T<sub>1/2</sub> value may be clinically advantageous. Oleuropein, Pinoreosinol, Apigenin, Hydroxytyrosol Toxicity and Metabolism Predictive Analyses were examined. The hERG encodes the pore-forming subunit of the rapidly activated delayed rectifier potassium channel, which is important for cardiac action

**Table 12** Predictive models parameters

		Hydroxytyrosol	Oleuropein	Apigenin	Pinoresinol
Physicochemical properties	Molecular Weight	154.16 g/mol	540.51 g/mol	270.24 g/mol	358.39 g/mol
	Formula	C8H10O3	C25H32O13	C15H10O5	C20H22O6
	Rotatable bonds	2	11	1	4
	H-bond acceptors	3	13	5	6
	H-bond donors	3	6	3	2
	Molar Refractivity	41.42	127.28	73.99	94.90
	Topological polar surface area (TPSA)	60.69 Å <sup>2</sup>	201.67 Å <sup>2</sup>	90.90 Å <sup>2</sup>	77.38 Å <sup>2</sup>
Lipophilicity	Log Po/w (XLOGP3)	-0.72	-0.45	3.02	2.28
	Log P <sub>o/w</sub> (WLOGP)	0.63	-0.63	2.58	2.54
	Log P <sub>o/w</sub> (MLOGP)	0.60	-1.34	0.52	1.17
Solubility	Log S (ESOL)	-0.61	-2.30	-3.94	-3.58
	Solubility (water)	3.75e+01 mg/ml; 2.43e-01 mol/l	2.72e+00 mg/ml; 5.03e-03 mol/l	3.07e-02 mg/ml; 1.14e-04 mol/l	9.52e-02 mg/ml; 2.66e-04 mol/l
Druglikeness	Class	Very soluble	Soluble	Soluble	Soluble
	Lipinski (RO5)	Yes; 0 violation	No; 3 violations: MW > 500, NorO > 10, NHorOH > 5	Yes; 0 violation	Yes; 0 violation
	Ghose	No; 1 violation: MW < 160	No; 2 violations: MW > 480, WLOGP < -0.4	Yes	Yes
	Veber	Yes	No; 2 violations: Rotors > 10, TPSA > 140	Yes	Yes
	Egan	Yes	No; 1 violation: TPSA > 131.6	Yes	Yes
	Bioavailability Score	0.55	0.11	0.55	0.55
Leadlikeness	Synthetic accessibility	1.08	6.22	2.96	3.99

**Table 13** The interaction of hydroxytyrosol, oleuropein, apigenin, pinoresinol with cytochromes P450 isoforms predicted using SwissADME

Pharmacokinetics parameters		Hydroxytyrosol	Oleuropein	Apigenin	Pinoresinol
Pharmacokinetics	GI absorption	High	Low	High	High
	BBB permeant	No	No	No	Yes
	P-gp substrate	No	Yes	No	Yes
	CYP1A2 inhibitor	No	No	Yes	No
	CYP2C9 inhibitor	No	No	No	No
	CYP2C19 inhibitor	No	No	No	No
	CYP3A4 inhibitor	No	No	Yes	Yes
	CYP2D6 inhibitor	No	No	Yes	Yes
	Log Kp (skin permeation)	-7.75 cm/s	-9.92 cm/s	-5.80 cm/s	-6.87 cm/s

GI (HIA) human gastrointestinal absorption, BBB blood-brain barrier permeation, P-gp permeability glycoprotein, Log Kp the skin permeability coefficient

**Table 14** Absorption, distribution and excretion parameters of the Hydroxytyrosol, Oleuropein, Apigenin, Pinoresinol

Molecule	Absorption						Distribution			Excretion	
	Caco-2	Pgp inh	Pgp sub	HIA	F20	F30	PPB (%)	BBB	VD	T1/2	TCL
Hydroxytyrosol	-4.43	--	--	++	+++	+++	35.53	--	1.12	0.9	17.2
Oleuropein	-5.8	--	++	+++	-	+++	74.00	+	0.56	0.83	2.5
Apigenin	-4.84	--	++	--	+++	+++	97.25	--	0.51	0.85	7.02
Pinoresinol	-4.79	--	--	--	--	--	94.77	-	1.05	0.43	7.89

potential repolarization. Dysfunction of these ion channels causes cardiac arrhythmias and sudden death. When the findings were examined, the hERG values of Hydroxytyrosol, Oleuropein, Apigenin, Pinoresinol were not significant (Table 15). [101, 102].

Drug-induced liver injury (DILI) assessment is an important parameter to determine the potential toxic effect of a molecule on the liver. The higher the DILI value, the higher the potential for that molecule to cause damage to the liver. The high DILI value of apigenin means that this compound can exert more toxic effects on the liver. On the other hand, the low DILI value of Hydroxytyrosol indicates that this molecule has less toxic effects on the liver. Therefore, while Hydroxytyrosol may be a safer compound for the liver, the interpretation that its therapeutic use may offer a safer profile comes to mind [103] (Table 15). As a result of Carcinogenicity and AMES toxicity, Oleuropein is the highest. The environmental toxicity profile bioconcentration factors are IGC50, LC50FM and LC50DM (Table 15) [104]. Only the Oleuropein Genotoxic Carcinogenicity Rule 1 provided alerts when the toxicophore rules were analyzed. Other than that, the other components were insignificant (Table 15).

In Fig. 9 the ESP maps of the compounds were also given. The notion of the electrostatic potential (ESP) is essential to density functional theory (DFT) calculations because it captures the complex electron–electron interactions and electron density distribution in a system. Theoretically, ESP contributes significantly to our understanding of electronic structure and molecular energetics as well as material characteristics. Positive regions were shown in blue or green on ESP maps produced from DFT calculations, whereas negative regions were shown in red or orange. The distribution of electron density in molecules or materials can be better seen with the use of these colors. Molecular orbital theory was used to investigate chemical stability and reactivity. Furthermore, the energy values of the HOMO and LUMO were used to calculate the quantum reactivity parameters. The negative areas indicate areas with relatively higher electron densities, indicating an environment rich in electrons or

an abundance of electrons. These regions usually correspond to electron-rich functional groups, such as lone pairs of electrons or  $\pi$ -electron systems in organic compounds. Chemically, locations of potential electron donation or nucleophilic activity are connected to negative areas. The component of global electrophilicity shows how effectively electron acceptors can pick up additional electronic charge from the system [105–108].

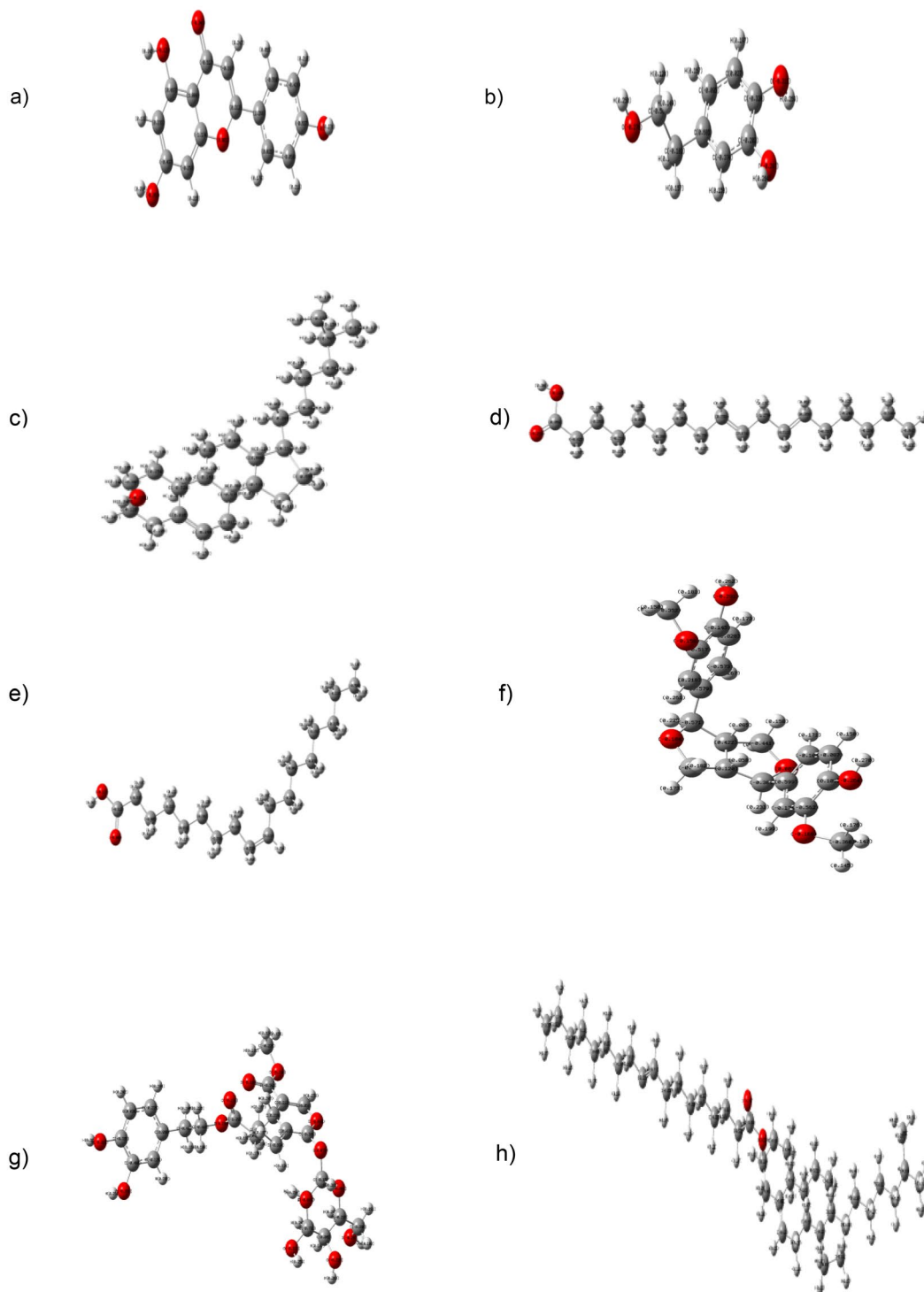
Positive zones on ESP maps, on the other hand, indicate lower electron densities and thus electron-deficient or electron-poor settings. These regions are usually found near electrophilic functional groups or atoms with much higher electronegativity than their adjacent atoms. Electrophilic behavior, in which molecules or atoms attempt to take electrons from other species, is typically associated with positive regions. In the ESP (Electrostatic Potential) analysis of the molecular structures provided, it has been observed that regions containing oxygen atoms exhibit negative charge [109–112]. This observation is consistent across the compounds (a) Apigenin, (b) Hydroxytyrosol, (d) Linoleic Acid, (e) Oleic Acid, (f) Pinoresinol, and (g) Oleuropein. In these molecules, oxygen atoms typically participate in electron-rich functional groups such as hydroxyl (-OH) or carbonyl (C=O) moieties. These oxygen-containing groups contribute to the overall negative electrostatic potential due to their ability to attract electrons. This characteristic is significant in understanding the chemical reactivity and intermolecular interactions of these compounds, particularly in contexts such as hydrogen bonding or interaction with positively charged species. Furthermore, the existence of negative ESP areas surrounding oxygen atoms may have an impact on the compounds' stability, solubility, or biological activity in different environments [113–115]. Cholesterol and Cholesterol-Oleic Acid may exhibit different reactivity characteristics due to their distinct molecular compositions and functional groups, suggesting potential variations in their electrostatic profiles and reactivity patterns.

Furthermore, Table 16 presented clear correlations between the dipole moments of the molecules and their corresponding chemical attributes, including spatial

**Table 15** Toxicity parameters of the hydroxytyrosol, oleuropein, apigenin, pinoresinol

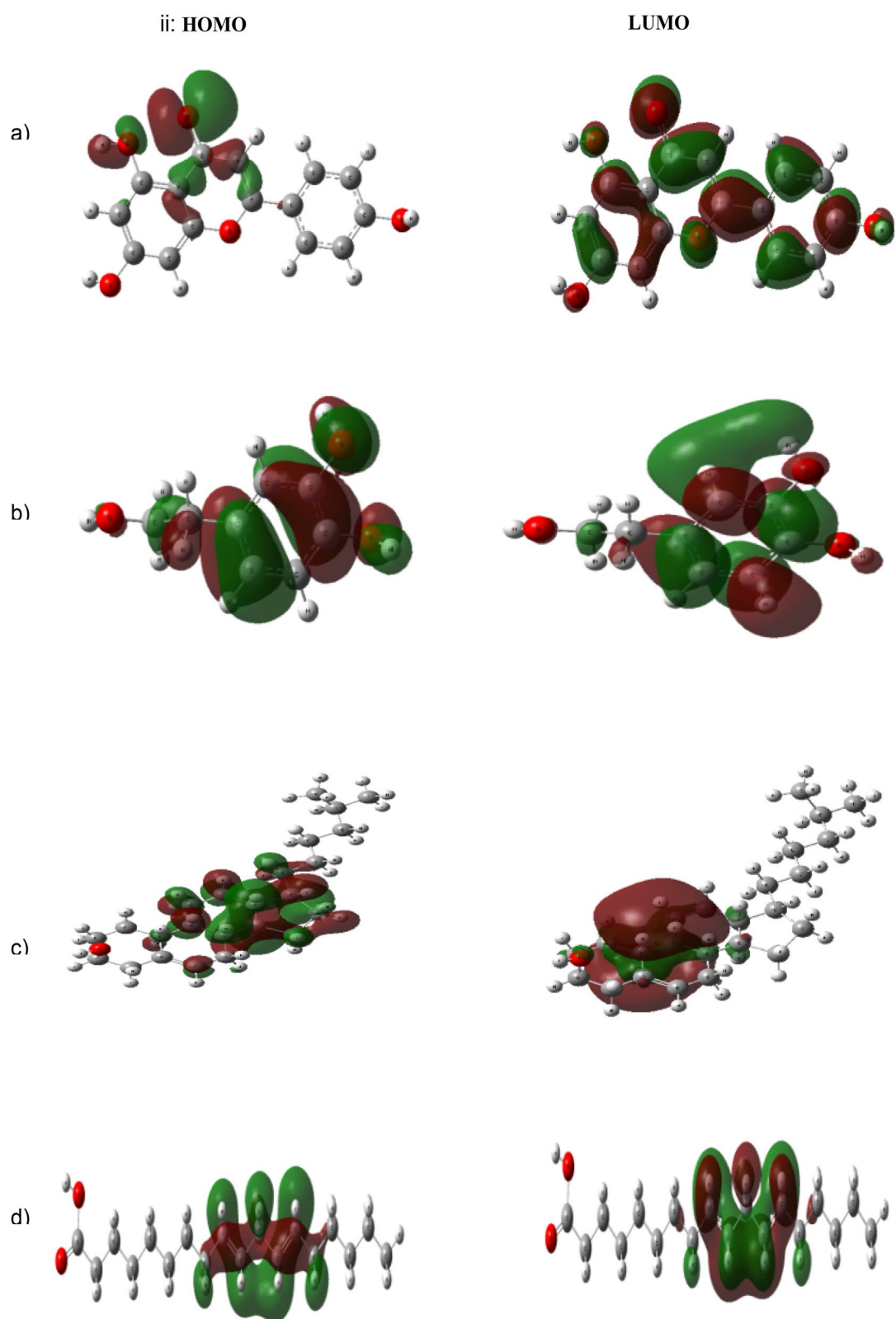
Molecule	Toxicity						Environmental toxicity			Toxicophore rules	
	hERG	H-HT	AMES Tox	SkinSen	DILI	Carcinogenicity	IGC50	LC50FM	LC50DM	Acute toxicity rule	Genotoxic carcinogenicity rule
Hydroxytyrosol	--	--	+	++	--	-	3.03	3.29	4.26	0 Alert(s)	0 Alert(s)
Oleuropein	--	-	++	--	+++	+++	3.52	4.5	5.38	0 Alert(s)	1 Alert(s)
Apigenin	--	--	-	+++	++	-	4.58	5.20	5.20	0 Alert(s)	0 Alert(s)
Pinoresinol	--	-	-	+	-	-	5.02	5.80	6.63	0 Alert(s)	0 Alert(s)

## i. Mulliken



**Fig. 9** Compounds structures of (a) Apigenin, (b) Hydroxytyrosol, (c) Cholesterol, (d) Linoleic Acid, (e) Oleic Acid, (f) Pinoresinol, (g) Oleuropein and (h) Cholesterol-Oleic Acid (i: Mulliken charges; ii: HOMO and LUMO; iii: ESP)



**Fig. 9** continued

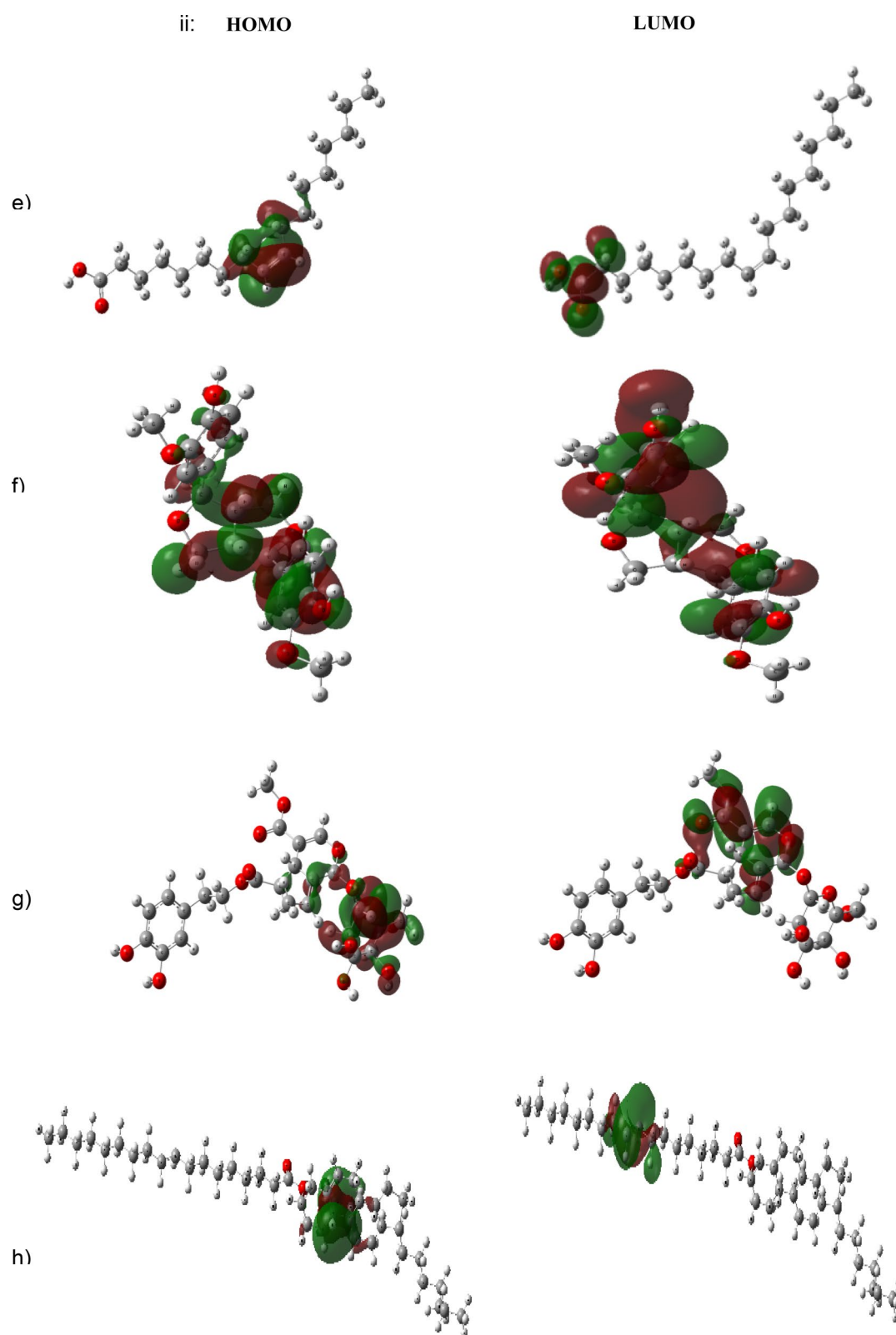


Fig. 9 continued

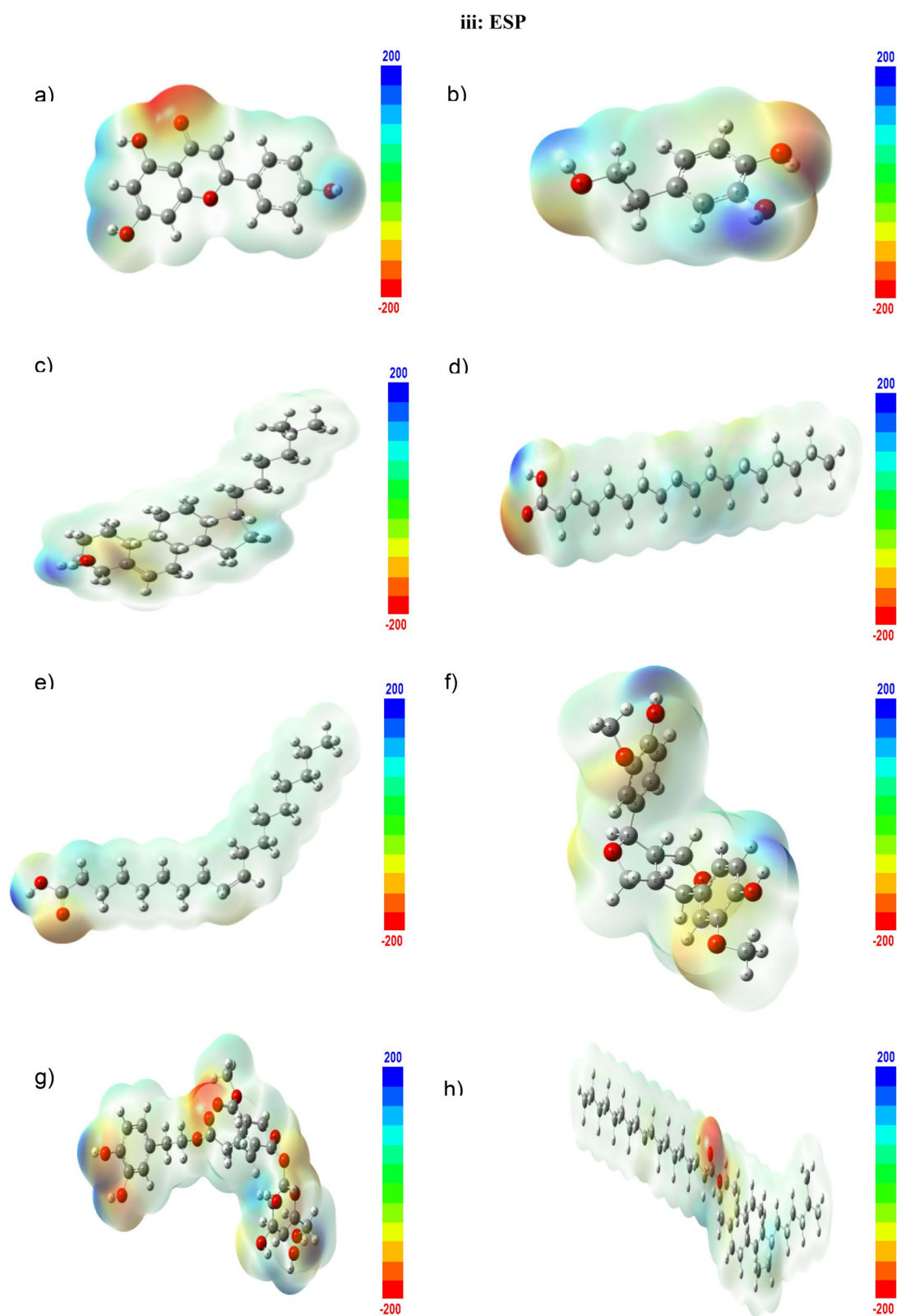


Fig. 9 continued

**Table 16** The calculated quantum parameters for oleic acid, linoleic acid, cholesterol, hydroxytyrosol, apigenin, pinorelinol, oleuropein and cholesterol-oleic acid, by DFT/B3LYP/6-311G (+ + d,p) method

Molecule/compound	$E_{\text{HOMO}}$ (eV)	$E_{\text{LUMO}}$ (eV)	$\Delta E$ (eV)	$\chi$ (eV)	$\eta$ (eV)	$s$ (eV <sup>-1</sup> )	Total energy (au)	$\mu$ (Debye)
Oleic acid	-6.02	-1.73	4.28	3.88	2.14	0.46	-856.9	3.86
Linoleic acid	-5.65	-3.27	2.38	4.46	1.19	0.84	-855.5	3.26
Cholesterol	-3.79	-0.60	3.18	2.20	1.59	0.62	-1013.7	1.90
Hydroxytyrosol	-6.62	-7.91	-1.28	7.26	-0.64	-1.55	-536.6	1.40
Apigenin	-5.94	-2.56	3.37	4.25	1.68	0.59	-953.9	4.22
Pinorelinol	-5.78	-0.85	4.93	3.31	2.46	0.40	-1226.6	4.30
Oleuropein	-6.04	-2.15	3.89	4.09	1.94	0.51	-1949.2	6.10
Cholesterol_Oleic acid	-3.95	-2.76	1.19	3.35	0.59	1.67	-1794.2	2.88

arrangement and electronic structure. The distribution of charge within a molecule is reflected by the dipole moment, which is a measure of polarity and is controlled by molecular geometry and the electronegativity of constituent atoms. In Table 16, compounds with stronger dipole moments, such as oleuropein and pinorelinol, typically have more polar bonds or asymmetric chemical structures, which cause the positive and negative charges to be significantly separated along the molecular axis. This is in line with their chemical structures, where the unequal electron sharing caused by strongly electronegative atoms—like oxygen in pinorelinol and numerous oxygen atoms in oleuropein—contributes to prominent dipole moments. The molecules with smaller dipole moments, such as hydroxytyrosol and cholesterol, may exhibit more symmetric molecular structures or have less polar bonds, resulting in a reduced separation of charges and hence smaller dipole moments. This is evident in their molecular compositions, where the distribution of electronegative atoms and the overall symmetry of the molecule contribute to relatively lower dipole moments compared to more polar compounds. The relationship between dipole moment and molecular properties can also be inferred from the  $E_{\text{HOMO}}$  and  $E_{\text{LUMO}}$ , as well as the total energy changes upon compound formation. Higher dipole moments are often associated with molecules possessing larger energy gaps between  $E_{\text{HOMO}}$  and  $E_{\text{LUMO}}$ , indicative of stronger intramolecular charge transfer and greater polarity.

The total energy changes upon the formation of compounds involving cholesterol and oleic acid can provide valuable insights into their stability and interactions. When considering the individual components, cholesterol and oleic acid, they possess distinct total energy values, reflecting their respective molecular structures and electronic configurations. However, upon combining these molecules to form cholesterol-oleic acid, there is a discernible alteration (diminishing) in the total

energy, indicating the stable new molecular entities. This drop indicates a strengthening of the intermolecular interactions, most likely due to the creation of chemical bonds between the constituent molecules and favorable molecular conformations. Enlightening the energetics of molecular contacts and the production of molecules of biological significance, the overall energy changes provide information on the thermodynamic probability and stability of the reaction between oleic acid and cholesterol.

## Conclusions

In this study, both experimental and computational results provide complementary insights, aligning to reinforce the observed properties of key phenolic compounds in EVOO. The molecular docking analysis highlighted strong binding affinities of apigenin and pinorelinol to target proteins, corroborating their known pharmacological potential, particularly in cardiovascular health. The ADMET analysis aligns well with experimental observations on bioavailability; hydroxytyrosol and apigenin, both with higher bioavailability and absorption potential, match previously reported data on their effective absorption and therapeutic use. The DFT findings, including dipole moments and molecular structure support the pharmacokinetic advantages of hydroxytyrosol, apigenin, and pinorelinol, as these molecules exhibit suitable molecular sizes and stable interactions.

In the toxicity analysis, while the hERG values of all components were not found to be significant, it indicates that the risk of cardiac toxicity of these components is low. Apigenin may cause more damage to the liver with a high DILI value, while Hydroxytyrosol may be safer for the liver with a low DILI value.

Additionally, KEGG enrichment analysis of these compounds demonstrated correlations with lipid metabolism and atherosclerosis, consistent with experimental studies on EVOO's health benefits.



Overall, the computational insights reinforce the experimental observations, providing a more comprehensive understanding of the therapeutic potential and safety of these compounds.

#### Abbreviations

CVD	Cardiovascular diseases
DFT	Density functional theory
DILI	Drug-induced liver injury
EVOO	Extra virgin olive oil
FA	Fatty acids
GC-FID	Gas chromatography flame ionization detector
HERG	The human ether-a-go-go-related gene
HIA	Human intestinal absorption
KEEG	Kyoto Encyclopedia of Genes and Genomes
PC	Phenolic compounds
SAM	Sulbactam/ampicillin
SPME	Solid phase micro extraction
TPC	Total phenolic content
TAC	Total antioxidant capacity
TE	Trolox equivalents
VC	Volatile compounds

#### Acknowledgements

None.

#### Author contributions

Velid Unsal: Project administration, Formal analysis, Conceptualization, Investigation, Methodology, Supervision, Visualization, Writing—original draft, Writing—review and editing. Reşit Yıldız: Investigation, Methodology, Writing—original draft. Aziz Korkmaz: Methodology, Formal analysis, Writing—review and editing. Başak Doğru Mert: Investigation, Methodology, Data curation, Writing—review and editing. Cemile Gunbegi Caliskan: Methodology, Writing—review and editing. Erkan Oner: Conceptualization, Investigation, Methodology, Writing—review and editing.

#### Funding

None.

#### Data availability

The datasets used and/or analysed during the current study are available from the corresponding author on reasonable request.

#### Declarations

##### Ethics approval and consent to participate

The "informed consent to participate" was obtained from the owner of the garden for the study.

##### Consent for publication

Not applicable in this section.

##### Competing interests

The authors declare no competing interests.

Received: 19 September 2024 Accepted: 20 December 2024

Published online: 03 January 2025

#### References

- Rossi R. The Eu olive and olive oil sector main features, challenges and prospects. European Parliamentary Research Service; European Parliament: Brussels, Belgium, 12. 2017.
- Jimenez-Lopez C, Carpena M, Lourenço-Lopes C, Gallardo-Gomez M, Lorenzo JM, Barba FJ, et al. Bioactive compounds and quality of extra virgin olive oil. *Foods*. 2020;9(8):1014.
- Korkmaz A. Characterization and comparison of extra virgin olive oils of turkish olive cultivars. *Molecules*. 2023;28(3):1483.
- Veneziani G, Esposito S, Taticchi A, Urbani S, Selvaggini R, Sordini B, Servili M. Characterization of phenolic and volatile composition of extra virgin olive oil extracted from six Italian cultivars using a cooling treatment of olive paste. *LWT*. 2018;87:523–8.
- De Santis S, Cariello M, Piccinin E, Sabbà C, Moschetta A. Extra virgin olive oil: lesson from nutrigenomics. *Nutrients*. 2019;11(9):2085.
- Franconi F, Campesi I, Romani A. Is extra virgin olive oil an ally for women's and men's cardiovascular health? *Cardiovasc Therapeut*. 2020;2020:1–33.
- Cicerale SRSJ, Lucas LJ, Keast RSJ. Antimicrobial, antioxidant and anti-inflammatory phenolic activities in extra virgin olive oil. *Curr Opin Biotechnol*. 2012;23(2):129–35.
- Cicerale S, Conlan XA, Sinclair AJ, Keast RS. Chemistry and health of olive oil phenolics. *Crit Rev Food Sci Nutr*. 2008;49(3):218–36.
- Seçmeler Ö, Galanakis CM. Olive fruit and olive oil. In: *Innovations in traditional foods*. UK: Woodhead Publishing; 2019. p. 193–220.
- Kouka P, Tsakiri G, Tzortzi D, Dimopoulou S, Sarikaki G, Stathopoulos P, Veskoukis AS, Halabalaki M, Skaltsounis AL, Kouretas D. The polyphenolic composition of extracts derived from different greek extra virgin olive oils is correlated with their antioxidant potency. *Oxid Med Cell Longev*. 2019;2019:1870965. <https://doi.org/10.1155/2019/1870965>.
- Kahraman G, Özkaya MT, Yildirim Ö. Potential anti-cancer effects of extra virgin olive oil and its phenolic extracts on hepatocellular carcinoma cells. *Int J Nat Life Sci*. 2023;7(2):112–22.
- Zhong F, Xing J, Li X, Liu X, Fu Z, Xiong Z, et al. Artificial intelligence in drug design. *Sci China Life Sci*. 2018;61:1191–204.
- Harrer S, Shah P, Antony B, Hu J. Artificial intelligence for clinical trial design. *Trends Pharmacol Sci*. 2019;40(8):577–91.
- Gupta R, Srivastava D, Sahu M, Tiwari S, Ambasta RK, Kumar P. Artificial intelligence to deep learning: machine intelligence approach for drug discovery. *Mol Diversity*. 2021;25:1315–60.
- International Olive Council (IOC). Guide for the Determination of the Characteristics of Oil-Olives. Available online: <https://www.internationaloliveoil.org/wp-content/uploads/2019/11/COI-OH-Doc.-1-2011-Eng.pdf>. 2011; Accessed 5 Nov 2023.
- Turkish Official Gazette. Available online: <https://www.resmigazete.gov.tr/eskiler/2014/11/20141120-21.htm>. Accessed 16 Sept 2024.
- International Olive Council (IOC). Available online: [https://www.internationaloliveoil.org/wp-content/uploads/2022/06/Doc.-No-29-REV-2\\_ENK.pdf](https://www.internationaloliveoil.org/wp-content/uploads/2022/06/Doc.-No-29-REV-2_ENK.pdf). Accessed 16 Sept 2024.
- Capanoglu E, De Vos RC, Hall RD, Boyacioglu D, Beekwilder J. Changes in polyphenol content during production of grape juice concentrate. *Food Chem*. 2013;139(1–4):521–6.
- Osei JB, Amiri A, Wang J, Tavares MT, Kiatkittipong W, Najdanovic-Visak V. Recovery of oils and antioxidants from olive stones. *Biomass Bioenerg*. 2022;166: 106623.
- Schlesier K, Harwat M, Bohm V, Bitsch R. Assessment of antioxidant activity by using different in vitro methods. *Free Radical Res*. 2002;36:177–87.
- Pirisi FM, Cabras P, Cao CF, Migliorini M, Muggelli M. Phenolic compounds in virgin olive oil. 2. Reappraisal of the extraction, HPLC separation, and quantification procedures. *J Agric Food Chem*. 2000;48(4):1191–6.
- Genovese A, Caporaso N, Sacchi R. Temporal changes of virgin olive oil volatile compounds in a model system simulating domestic consumption: the role of biophenols. *Food Res Int*. 2015;77:670–4.
- Wayne PA. NCCLS (National Committee for Clinical Laboratory Standards) performance standards for antimicrobial disk susceptibility tests: approved standard enclose-A 7. April 1997 ed. Wayne PA USA: NCCLS; 1997.
- Ercan L, Doğru M. Determination of antimicrobial activity of nasturtium officinale and its content of volatile organic compounds and fatty acids. *Kahramanmaraş Sütçü İmam Üniversitesi Tarım ve Doğa Dergisi*. 2022;25(Ek Sayı 1):11–21.
- Heberle H, Meirelles GV, da Silva FR, Telles GP, Minghim R. Inter-actiVenn: a web-based tool for the analysis of sets through Venn diagrams. *BMC Bioinformatics*. 2015;16(1):169. <https://doi.org/10.1186/s12859-015-0611-3>.

26. Storey JD. A direct approach to false discovery rates. *J R Stat Soc Ser B Stat Methodol.* 2002;64(3):479–98.
27. Yu G, Wang LG, Han Y, He QY. clusterProfiler: an R package for comparing biological themes among gene clusters. *Omics J Integr Biol.* 2012;16(5):284–7.
28. Biovia DS. Dassault systèmes BIOVIA, Discovery Studio, 2019, San Diego: Dassault Systèmes 2016.
29. Trott O, Olson AJ. AutoDock Vina: improving the speed and accuracy of docking with a new scoring function, efficient optimization, and multithreading. *J Comput Chem.* 2010;31:455–61.
30. Laskowski A, Mark B. LigPlot+: multiple ligand–protein interaction diagrams for drug discovery. *J Chem Inf Model.* 2011;51:2778–86.
31. Daina A. SwissADME: a free web tool to evaluate pharmacokinetics, drug-likeness and medicinal chemistry friendliness of small molecules. *Sci Rep.* 2017;7:42717.
32. Xiong G, Wu Z, Yi J, Fu L, Yang Z, Hsieh C, Yin M, Zeng X, Wu C, Lu A, Chen X, Hou T, Cao D. ADMETLab 2.0: an integrated online platform for accurate and comprehensive predictions of ADMET properties. *Nucleic Acids Res.* 2021;49(W1):W5–14. <https://doi.org/10.1093/nar/gkab255>.
33. Gaussian 09, Revision A.02, Frisch MJ, Trucks GW, Schlegel HB, Scuseria GE, Robb MA, Cheeseman JR, Scalmani G, Barone V, Petersson GA, Nakatsuji H, Li X, Caricato M, Marenich A, Bloino J, Janesko BG, Gomperts R, Mennucci B, Hratchian HP, Ortiz JV, Izmaylov AF, Sonnenberg JL, Williams-Young D, Ding F, Lipparini F, Egidi F, Goings J, Peng B, Petrone A, Henderson T, Ranasinghe D, Zakrzewski VG, Gao J, Rega N, Zheng G, Liang W, Hada M, Ehara M, Toyota K, Fukuda R, Hasegawa J, Ishida M, Nakajima T, Honda Y, Kitao O, Nakai H, Vreven T, Throssell K, Montgomery JA, Peralta JE, Ogliaro F, Bearpark M, Heyd JJ, Brothers E, Kudin KN, Staroverov VN, Keith T, Kobayashi R, Normand J, Raghavachari K, Rendell A, Burant JC, Iyengar SS, Tomasi J, Cossi M, Millam JM, Klene M, Adamo C, Cammi R, Ochterski JW, Martin RL, Morokuma K, Farkas O, Foresman JB, Fox DJ. Gaussian, Inc., Wallingford CT, 2016.
34. Selim A, Gökmen S, Resit Y, Mehmet FB. Protection of mild steel from corrosion in HCl solution via green Rumex acetosella extract: experimental and theoretical studies. *Mater Today Commun.* 2024;40: 109528.
35. Ökten V, Yıldız R, Sığırçık G. The adsorption and inhibition efficiency of 2-amino-4-methoxy-6-methyl-1,3,5-triazine for corrosion of mild steel in hydrochloric acid solution. *Anti-Corrosion Methods Mater.* 2023;70(6):350–60.
36. Keleşoğlu A, Yıldız R, Dehri İ. 1-(2-Hydroxyethyl)-2-imidazolidinone as corrosion inhibitor of mild steel in 0.5 M HCl solution: thermodynamic, electrochemical and theoretical studies. *J Adhesion Sci Technol.* 2019;33(18):2010–30.
37. Arslanhan S, Yıldız R, Döner A. Experimental and theoretical investigation of adsorption and inhibition properties of 2-Amino-1,3,5-triazine-4,6-dithiol against corrosion in hydrochloric acid solution on mild steel. *J Indian Chem Soc.* 2023;100: 101087.
38. Bitew M, Desalegn T, Demissie TB, Belayneh A, Endale M, Eswaramoorthy R. Pharmacokinetics and drug-likeness of antidiabetic flavonoids: molecular docking and DFT study. *PLoS ONE.* 2021;16(12): e0260853.
39. Primas H. Chemistry, quantum mechanics and reductionism: perspectives in theoretical chemistry. Cham: Springer Science & Business Media; 2013.
40. Unsal V, Yıldız R, Cicek M, Gungor M, Kurutas EB. Trans-chalcone attenuate arsenic-induced toxicity in 3T3 embryonic fibroblast cells; an in vitro and in silico study. *J Mol Struct.* 2024;1318: 139338.
41. Ismael M, Abdel-Mawgoud AMM, Rabia MK, Abdou A. Design and synthesis of three Fe (III) mixed-ligand complexes: exploration of their biological and phenoxazinone synthase-like activities. *Inorg Chim Acta.* 2020;505: 119443.
42. Barakat A, Soliman SM, Al-Majid AM, Lotfy G, Ghabbour HA, Fun HK, et al. Synthesis and structure investigation of novel pyrimidine-2,4,6-trione derivatives of highly potential biological activity as anti-diabetic agent. *J Mol Struct.* 2015;1098:365–76.
43. Stefanoudaki E, Williams M, Chartzoulakis K, Harwood J. Effect of irrigation on quality attributes of olive oil. *J Agric Food Chem.* 2009;57(15):7048–55.
44. European Commission. Regulation 1989/03 Amending Regulation (EEC) No 2568/91 on the Characteristics of Olive Oil and Olive-Pomace Oil and on the Relevant Methods of Analysis Modifies the CEE n. 2568/91 on Olive Oils and Pomace Olive Oils Characteristics and Relative Analysis Methods. Official Journal L. 295/57 13/11/2003 (2003)
45. Antonini E, Farina A, Leone A, Mazzara E, Urbani S, Selvaggini R, et al. Phenolic compounds and quality parameters of family farming versus protected designation of origin (PDO) extra-virgin olive oils. *J Food Compos Anal.* 2015;43:75–81.
46. Veneziani G, Esposito S, Taticchi A, Selvaggini R, Sordini B, Lorefice A, et al. Extra-virgin olive oil extracted using pulsed electric field technology: cultivar impact on oil yield and quality. *Front Nutr.* 2019;6:134.
47. Borges TH, Pereira JA, Cabrera-Vique C, Lara L, Oliveira AF, Seiquer I. Characterization of Arbequina virgin olive oils produced in different regions of Brazil and Spain: physicochemical properties, oxidative stability and fatty acid profile. *Food Chem.* 2017;215:454–62.
48. Lu Y, Zhao J, Xin Q, Yuan R, Miao Y, Yang M, et al. Protective effects of oleic acid and polyphenols in extra virgin olive oil on cardiovascular diseases. *Food Sci Human Wellness.* 2024;13(2):529–40.
49. Teres S, Barceló-Coblijn G, Benet M, Alvarez R, Bressani R, Halver JE, Escriba PV. Oleic acid content is responsible for the reduction in blood pressure induced by olive oil. *Proc Natl Acad Sci.* 2008;105(37):13811–6.
50. Serrelli G, Deiana M. Extra virgin olive oil polyphenols: modulation of cellular pathways related to oxidant species and inflammation in aging. *Cells.* 2020;9(2):478.
51. Caramia G, Gori A, Valli E, Cerretani L. Virgin olive oil in preventive medicine: from legend to epigenetics. *Eur J Lipid Sci Technol.* 2012;114:375–88.
52. López-Miranda J, Pérez-Jiménez F, Ros E, De Caterina R, Badimón L, Covas MI, Escribá E, Ordovás JM, Soriguer F, Abiá R, et al. Olive oil and health: summary of the II international conference on olive oil and health consensus report, Jaén and Córdoba (Spain) 2008. *Nutr Metab Cardiovasc Dis.* 2010;20:284–94.
53. Rodríguez-López P, Lozano-Sanchez J, Borrás-Linares I, Emanuelli T, Menéndez JA, Segura-Carretero A. Structure–biological activity relationships of extra-virgin olive oil phenolic compounds: health properties and bioavailability. *Antioxidants.* 2020;9(8):685.
54. Libby P. The changing landscape of atherosclerosis. *Nature.* 2021;592(7855):524–33.
55. Roth GA, Mensah GA, Johnson CO, Addolorato G, Ammirati E, Baddour LM, et al. Global burden of cardiovascular diseases and risk factors, 1990–2019: update from the GBD 2019 study. *J Am Coll Cardiol.* 2020;76(25):2982–3021.
56. Heidenreich PA, Trogdon JG, Khavjou OA, Butler J, Dracup K, Ezekowitz MD, et al. Forecasting the future of cardiovascular disease in the United States: a policy statement from the American Heart Association. *Circulation.* 2011;123(8):933–44.
57. McConnachie A, Walker A, Robertson M, Marchbank L, Peacock J, Packard CJ, et al. Long-term impact on healthcare resource utilization of statin treatment, and its cost effectiveness in the primary prevention of cardiovascular disease: a record linkage study. *Eur Heart J.* 2014;35(5):290–8.
58. Libby P, Buring JE, Badimón L, et al. Atherosclerosis. *Nat Rev Dis Primers.* 2019;5:56. <https://doi.org/10.1038/s41572-019-0106->
59. De Meyer GR, Zurek M, Puylaert P, Martinet W. Programmed death of macrophages in atherosclerosis: mechanisms and therapeutic targets. *Nat Rev Cardiol.* 2024;21:312.
60. Nocella C, Cammisotto V, Fianchini L, D'Amico A, Novo M, Castellani V, et al. Extra virgin olive oil and cardiovascular diseases: benefits for human health. *Endocr Metab Immune Disord Drug Targets.* 2018;18(1):4–13.
61. Mazzocchi A, Leone L, Agostoni C, Pali-Schöll I. The secrets of the Mediterranean diet. Does [only] olive oil matter? *Nutrients.* 2019;11(12):2941.
62. López-Yerena A, Lozano-Castellón J, Olmo-Cunillera A, Tresserra-Rimbau A, Quifer-Rada P, Jiménez B, et al. Effects of organic and conventional growing systems on the phenolic profile of extra-virgin olive oil. *Molecules.* 2019;24(10):1986.
63. Piroddi M, Albini A, Fabiani R, Giovannelli L, Luceri C, Natella F, et al. Nutrigenomics of extra-virgin olive oil: a review. *BioFactors.* 2017;43(1):17–41.
64. Rigacci S, Stefani M. Nutraceutical properties of olive oil polyphenols. An itinerary from cultured cells through animal models to humans. *Int J Mol Sci.* 2016;17(6):843.

65. Karković Marković A, Torić J, Barbarić M, Jakobušić BC. Hydroxytyrosol, tyrosol and derivatives and their potential effects on human health. *Molecules*. 2019;24(10):2001.
66. Li W, Chountoules M, Antoniadi L, Angelis A, Lei J, Halabalaki M, et al. Development and physicochemical characterization of nanoliposomes with incorporated oleocanthal, oleacein, oleuropein and hydroxytyrosol. *Food Chem*. 2022;384: 132470.
67. Omar SH. Cardioprotective and neuroprotective roles of oleuropein in olive. *Saudi Pharmaceut J*. 2010;18(3):111–21.
68. Shamshoum H, Vlavcheski F, Tsiani E. Anticancer effects of oleuropein. *BioFactors*. 2017;43(4):517–28.
69. García-Martínez O, De Luna-Bertos E, Ramos-Torrecillas J, Ruiz C, Milia E, Lorenzo ML, et al. Phenolic compounds in extra virgin olive oil stimulate human osteoblastic cell proliferation. *PLoS ONE*. 2016;11(3): e0150045.
70. Noguera-Navarro C, Montoro-García S, Orenes-Piñero E. Hydroxytyrosol: its role in the prevention of cardiovascular diseases. *Heliyon*. 2023;9(1): e12963.
71. Di Benedetto R, Vari R, Scaccocchio B, Filesi C, Santangelo C, Giovannini C, et al. Tyrosol, the major extra virgin olive oil compound, restored intracellular antioxidant defenses in spite of its weak antioxidative effectiveness. *Nutr Metab Cardiovasc Dis*. 2007;17(7):535–45.
72. Xu Y, Li X, Wang H. Protective roles of apigenin against cardiometabolic diseases: a systematic review. *Front Nutr*. 2022;9: 875826.
73. Karagoz SG, Yilmazer M, Ozkan G, Carbonell-Barrachina AA, Kiralan M, Ramadan MF. Effect of cultivar and harvest time on C6 and C5 volatile compounds of Turkish olive oils. *Eur Food Res Technol*. 2017;243(7):1193–200. <https://doi.org/10.1007/s00217-016-2833-7>.
74. Ozcan-Sinir G. Detection of adulteration in extra virgin olive oil by selected ion flow tube mass spectrometry (SIFT-MS) and chemometrics. *Food Control*. 2020;118: 107433. <https://doi.org/10.1016/j.foodcont.2020.107433>.
75. Giuffrè AM, Capocasale M, Macrì R, Caracciolo M, Zappia C, Poiana M. Volatile profiles of extra virgin olive oil, olive pomace oil, soybean oil and palm oil in different heating conditions. *LWT*. 2020;117: 108631. <https://doi.org/10.1016/j.lwt.2019.108631>.
76. Marx IMG, Casal S, Rodrigues N, Cruz R, Peres F, Veloso ACA, Pereira JA, Peres AM. Impact of fresh olive leaves addition during the extraction of Arbequina virgin olive oils on the phenolic and volatile profiles. *Food Chem*. 2022;393: 133327. <https://doi.org/10.1016/j.foodchem.2022.133327>.
77. Spadafora ND, Mascres S, McGregor L, Purcaro G. Exploring multiple-cumulative trapping solid-phase microextraction coupled to gas chromatography–mass spectrometry for quality and authenticity assessment of olive oil. *Food Chem*. 2022;383: 132438. <https://doi.org/10.1016/j.foodchem.2022.132438>.
78. Restuccia D, Clodoveo ML, Corbo F, Loizzo MR. De-stoning technology for improving olive oil nutritional and sensory features: the right idea at the wrong time. *Food Res Int*. 2018;106:636–46. <https://doi.org/10.1016/j.foodres.2018.01.043>.
79. Bertuccioli M, Monteleone E. The sensory quality of extra-virgin olive oil. In: Peri C, editor. *The extra-virgin olive oil handbook*. Hoboken: Wiley; 2014. p. 35–58.
80. IOC (2018) Sensory Analysis of Olive Oil Method for the Organoleptic Assessment of Virgin Olive Oil. COI/T.20/Doc. No 15/Rev. 10. 2018. Available online: <https://www.internationaloliveoil.org/wp-content/uploads/2019/11/COI-T20-Doc-15-REV-10-2018-Eng.pdf>. Accessed 26 Jun 2024.
81. Mariotti M. Virgin olive oil: definition. In: Peri C, editor. *The Extra-virgin olive oil handbook*. Hoboken: Wiley; 2014. p. 11–9.
82. Zhang M, Li Q, Yu D, Yao B, Guo W, Xie Y, Xiao G. GeNeCK: a web server for gene network construction and visualization. *BMC Bioinformatics*. 2019;20:1–7.
83. Bernstein KE, Khan Z, Giani JF, Cao DY, Bernstein EA, Shen XZ. Angiotensin-converting enzyme in innate and adaptive immunity. *Nat Rev Nephrol*. 2018;14(5):325–36. <https://doi.org/10.1038/nrneph.2018.15>.
84. Miller AJ, Arnold AC. The renin-angiotensin system in cardiovascular autonomic control: recent developments and clinical implications. *Clin Auton Res*. 2019;29(2):231–43. <https://doi.org/10.1007/s10286-018-0572-5>.
85. Azushima K, Morisawa N, Tamura K, Nishiyama A. Recent research advances in renin–angiotensin–aldosterone system receptors. *Curr Hypertens Rep*. 2020;22(3):22. <https://doi.org/10.1007/s11906-020-1028-6>.
86. Kamo T, Akazawa H, Komuro I. Pleiotropic effects of angiotensin II receptor signaling in cardiovascular homeostasis and aging. *Int Heart J*. 2015;56(3):249–54. <https://doi.org/10.1536/ihj.14-429>.
87. Tóth AD, Turu G, Hunyady L, Balla A. Novel mechanisms of G-protein-coupled receptors functions: AT1 angiotensin receptor acts as a signaling hub and focal point of receptor cross-talk. *Best Pract Res Clin Endocrinol Metab*. 2018;32(2):69–82. <https://doi.org/10.1016/j.beem.2018.02.003>.
88. Higuchi S, Ohtsu H, Suzuki H, Shirai H, Frank GD, Eguchi S. Angiotensin II signal transduction through the AT1 receptor: novel insights into mechanisms and pathophysiology. *Clin Sci (London, England)*. 2007;112(8):417–28. <https://doi.org/10.1042/CS20060342>.
89. Karnik SS, Unal H, Kemp JR, Tirupula KC, Eguchi S, Vanderheyden PM, Thomas WG. International union of basic and clinical pharmacology. XCIX. Angiotensin receptors: interpreters of pathophysiological angiotensinergic stimuli [corrected]. *Pharmacol Rev*. 2015;67(4):754–819. <https://doi.org/10.1124/pr.114.010454>.
90. Wang Y, Fan Z, Xu C, Yan X, Zhou Y, Qiu Z, Yuan Q, Zheng J, Yuhua Liao Y, Chen X. Anti-ATR001 monoclonal antibody ameliorates atherosclerosis through beta-arrestin2 pathway. *Biochem Biophys Res Commun*. 2021;544:1–7. <https://doi.org/10.1016/j.bbrc.2021.01.054>.
91. Singh KD, Karnik SS. Angiotensin receptors: structure, function, signaling and clinical applications. *J Cell Signal*. 2016;1(2):111. <https://doi.org/10.4172/jcs.1000111>.
92. Pires DEV, Blundell TL, Ascher DB. pkCSM: predicting smallmolecule pharmacokinetic and toxicity properties using graph-based signatures. *J Med Chem*. 2018;58(9):4066–72.
93. Cheng F, Li W, Zhou Y, Shen J, Wu Z, Liu G, Lee PW, Tang Y. admetSAR: a comprehensive source and free tool for assessment of chemical ADMET properties. *J Chem Inf Model*. 2012;52(11):3099–105.
94. Lynch T, Price AMY. The effect of cytochrome P450 metabolism on drug response, interactions, and adverse effects. *Am Fam Physician*. 2007;76(3):391–6.
95. Hakkola J, Hukkanen J, Turpeinen M, Pelkonen O. Inhibition and induction of CYP enzymes in humans: an update. *Arch Toxicol*. 2020;94:3671–722.
96. Van De Waterbeemd H, Gifford E. ADMET in silico modelling: towards prediction paradise? *Nat Rev Drug Discov*. 2003;2(3):192–204.
97. Croom E. Metabolism of xenobiotics of human environments. *Prog Mol Biol Transl Sci*. 2012;112:31–88.
98. Golan DE, et al. *Principios de Farmacología*. Guanabara Koogan, 2014, 2 edn.
99. Smith DA, Beaumont K, Maurer TS, Di L. Volume of distribution in drug design. *J Med Chem*. 2015;58(15):5691–8.
100. Mansoor A, Mahabadi N. Volume of distribution. [Updated 2023 Jul 24]. In: *StatPearls*. Treasure Island (FL): StatPearls Publishing; 2024 Jan. Available from: <https://www.ncbi.nlm.nih.gov/books/NBK545280/>.
101. Lamothe SM, Guo J, Li W, Yang T, Zhang S. The human ether-a-go-go-related gene (hERG) potassium channel represents an unusual target for protease-mediated damage. *J Biol Chem*. 2016;291(39):20387–401.
102. Butler A, Helliwell MV, Zhang Y, Hancox JC, Dempsey CE. An update on the structure of hERG. *Front Pharmacol*. 2020;10:1572.
103. Bessone F, Hernandez N, Tagle M, Arrese M, Parana R, Mendez-Sánchez N, et al. Drug-induced liver injury: a management position paper from the Latin American Association for Study of the liver. *Ann Hepatol*. 2021;24:100321.
104. Gandla K, Islam F, Zehravi M, Karunakaran A, Sharma I, Haque MA, Kumar S, Pratyush K, Dhawale SA, Nainu F, Khan SL, Islam MR, Al-Mugren KS, Siddiqui FA, Emran TB, Khandaker MU. Natural polymers as potential P-glycoprotein inhibitors: pre-ADMET profile and computational analysis as a proof of concept to fight multidrug resistance in cancer. *Heliyon*. 2023;9(9): e19454.
105. Zahra P, Ghodsi Mohammadi Z, Mehran F, Alireza B, Ahmed MA. Synthesis and DFT calculation of Hg<sup>2+</sup> fluorescence chemosensor based on a new hybrid organic–inorganic nanoporous material of SBA-Pr-Is-Hy. *Appl Organometall Chem*. 2024:e7818.
106. Touhami L, Mehran F, Elhafaoui L. Assessment of the electrostatic binding of ferrocenylmethyl-nitroaniline derivatives to DNA: a

- combined experimental and theoretical study. *J Mol Struct.* 2024;1308: 138386.
107. Velichka A, Krastena N, Ivelin I, Svetlana G, Mehran F, Stoyanka N, Anelia G. Spectral characteristics, in silico perspectives, density functional theory (DFT), and therapeutic potential of green-extracted phycocyanin from spirulina. *Int J Mol Sci.* 2024;25:9170.
  108. Ghodsi MZ, Mahtab R, Mehran F, Stoyanka N. Fumed-Si-Pr-Ald-Barb as a fluorescent chemosensor for the Hg<sup>2+</sup> detection and Cr<sub>2</sub>O<sub>7</sub><sup>2-</sup> ions: a combined experimental and computational perspective. *Molecules.* 2024;29:4825.
  109. Chai YM, Zhang HB, Zhang XY, Chai LQ. X-ray structures, spectroscopic, antimicrobial activity, ESP/HSA and TD/DFT calculations of Bi (III) complex containing imidazole ring. *J Mol Struct.* 2022;1256: 132517.
  110. An HL, Duan Y, Chen TT, Chai LQ. Experimental and theoretical studies of trinuclear cadmium (II) complex containing pyridine ring: synthesis, crystallographic, spectroscopic, TD/DFT calculations and Hirshfeld surface analysis. *J Mol Struct.* 2024;1310: 138320.
  111. Majumdar D, Roy S, Philip JE, Tüzün B, Hazra S. In-situ Salen-type ligand formation-driven of a heterometallic Cu (II)-Hg (II) complex: synthetic update, crystallographic features, DFT calculations, and unveil antimicrobial profiles. *Inorg Chem Commun.* 2024;160: 111933.
  112. Wu C, Wang Y, Cai X, Wu Y, Du E, Zheng L, Peng M. Investigating haloacetic acids-human serum albumin interactions: a comprehensive approach using multi-spectroscopy, DFT calculations, and molecular docking. *J Mol Struct.* 2024;1299: 137143.
  113. Ahmed MA, Rafat ME, Tarek E, Mehran F, Ibrahim Omar B, Amal HA, Khalaf A, Abd El Aleem Ali M, Ali E. Design, preparation, physicochemical characterization, structural conformational, biological evaluation, and DNAinteraction for some new benzimidazole complexes. *Appl Organomet Chem.* 2024;38: e7358.
  114. Sahin D, Remziye AK, Mehran F, Senem A, José VC, Nicola M. Biological activities, DFT calculations, and molecular docking simulation of thymol-based compounds. *ChemistrySelect.* 2024;9: e202304572.
  115. Adnan Z, Selma F, Mehran F, Renata B, Amina K, Lora M, Aleksandar V, Anela T, Suncica R. Dual antimicrobial-anticancer potential, hydrolysis, and DNA/BSA binding affinity of a novel water-soluble ruthenium-arene ethylenediamine Schiff base (RAES) organometallic. *Spectrochim Acta Part A Mol Biomol Spectrosc.* 2024;318: 124528.

## Publisher's Note

Springer Nature remains neutral with regard to jurisdictional claims in published maps and institutional affiliations.